Department of Electrical Engineering and Automation

Adaptation luminance in a road lighting environment: analysis of non-uniform luminance distribution

Mikko Maksimainen

Aalto University

DOCTORAL DISSERTATIONS

Aalto University publication series
DOCTORAL DISSERTATIONS 172/2016

Adaptation luminance in a road lighting environment: analysis of non-uniform luminance distribution

Mikko Maksimainen

A doctoral dissertation completed for the degree of Doctor of Science (Technology) to be defended, with the permission of the Aalto University School of Electrical Engineering, at a public examination held at the lecture hall T2 of the school on the 25th of October 2016 at 12.

Aalto University
School of Electrical Engineering
Department of Electrical Engineering and Automation
Lighting Unit

Supervising professor
Prof. Liisa Halonen

Thesis advisors
Dr. Marjukka Puolakka
Dr. Eino Tetri

Preliminary examiners
Prof. Yandan Lin, Fudan University, China
Prof. Miyoshi Ayama, Utsunomiya University, Japan

Opponent
Prof. Stephan Völker, Technische Universität Berlin, Germany

Aalto University publication series
DOCTORAL DISSERTATIONS 172/2016

ISBN 978-952-60-6988-3 (printed)
ISBN 978-952-60-6987-6 (pdf)
ISSN-L 1799-4934
ISSN 1799-4934 (printed)
ISSN 1799-4942 (pdf)
http://urn.fi/URN:ISBN:978-952-60-6987-6

Unigrafia Oy
Helsinki 2016

Finland

441 697
Printed matter

Aalto University

Abstract

Aalto University, P.O. Box 11000, FI-00076 Aalto www.aalto.fi

Author
Mikko Maksimainen

Name of the doctoral dissertation
Adaptation luminance in a road lighting environment: analysis of non-uniform luminance distribution

Publisher School of Electrical Engineering

Unit Department of Electrical Engineering and Automation

Series Aalto University publication series DOCTORAL DISSERTATIONS 172/2016

Field of research Illumination

Manuscript submitted 19 May 2016 **Date of the defence** 25 October 2016

Permission to publish granted (date) 16 August 2016 **Language** English

☐ **Monograph** ☒ **Article dissertation** ☐ **Essay dissertation**

Abstract

In mesopic photometry, neither the scotopic $V'(\lambda)$ nor the photopic $V(\lambda)$ spectral luminous efficiency function solely applies. Instead, the spectral distribution of the luminaire and the adaptation state of the retina determine the mesopic spectral luminous efficiency function $V_{mes}(\lambda)$. The mesopic luminance region was defined as $0.005\ cdm^{-2}\ -\ 5\ cdm^{-2}$ by CIE (Commission Internationale de l'Eclairage) in 191:2010 System for mesopic photometry. However, the system for mesopic photometry cannot be fully utilised, until we have defined how to determine the state of adaptation – the adaptation luminance.

The aim of this work was to analyse the adaptation luminance in road lighting environment. Firstly, the test subjects' contrast thresholds within visual fields with non-uniform luminance distributions were examined. Secondly, the influence of disability glare sources on the adaptation luminance was quantified. Thirdly, a novel approach, where imaging luminance photometry is combined with 3D laser scanning, was examined.

Luminance non-uniformity clearly hindered the visual performance. The contrast threshold required for target detection could be 100% more on a luminously non-uniform background compared to a uniform background. The results also indicated that different retinal coordinates adapt independently to a local adaptation luminance.

In the street environment measurements, veiling luminance increased the adaptation luminance by 29% on average. Veiling luminance increases the adaptation luminance which shifts the spectral sensitivity in the retina towards photopic. This induced an average difference of $|0.6\%|$ in mesopic luminance calculation.

The observer's longitudinal location affects the adaptation luminance and the mesopic luminance in the measurement area. The location-dependent relative standard deviation among the calculated mesopic luminance values was 4.4%.

Combining luminance measurements to laser-scanned point clouds gave promising results. The method for the 3D location and luminance data integration was found successful.

In the field of lighting science, numerous further studies are needed before the adaptation luminance can be determined accurately. Firstly, no veiling luminance model can yet be utilised to an arbitrary retinal coordinate. Secondly, the effect of a constantly changing visual environment should be quantified. Thirdly, the physiological adaptation and the cognitive processing should be separated in terms of visual performance. In practical road lighting measurements though, the luminance in the measurement area can be a sufficient estimation for the adaptation luminance.

Keywords adaptation luminance, mesopic photometry, road lighting, disability glare

ISBN (printed) 978-952-60-6988-3 **ISBN (pdf)** 978-952-60-6987-6

ISSN-L 1799-4934 **ISSN (printed)** 1799-4934 **ISSN (pdf)** 1799-4942

Location of publisher Helsinki **Location of printing** Helsinki **Year** 2016

Pages 133 **urn** http://urn.fi/URN:ISBN:978-952-60-6987-6

Tekijä
Mikko Maksimainen

Väitöskirjan nimi
Adaptaatioluminanssi valaistussa tieympäristössä: epäyhtenäisen luminanssijakauman analyysi

Julkaisija Sähkötekniikan korkeakoulu

Yksikkö Sähkötekniikan ja automaation laitos

Sarja Aalto University publication series DOCTORAL DISSERTATIONS 172/2016

Tutkimusala Valaistustekniikka ja sähköinen talotekniikka

Käsikirjoituksen pvm 19.05.2016 **Väitöspäivä** 25.10.2016

Julkaisuluvan myöntämispäivä 16.08.2016 **Kieli** Englanti

☐ **Monografia** ☒ **Artikkeliväitöskirja** ☐ **Esseeväitöskirja**

Tiivistelmä

Sekä skotooppinen että fotoopinen spektriherkkyysfunktio ovat epäsopivia käytettäväksi mesooppisessa fotometriassa. Mesooppisen spektriherkkyysfunktion määrittämiseen tarvitaan valaisimen spektrijakauma sekä tieto havaitsijan verkkokalvon adaptaatiotilasta. CIE (Commission Internationale de l'Eclairage) määrittelee mesooppisen luminanssialueen olevan 0,005 cdm^{-2} – 5 cdm^{-2} raportissa '191:2010 System for mesopic photometry.' Tätä mesooppisen fotometrian järjestelmää ei kuitenkaan voi täysin käyttää, ennen kuin on rajattu kuinka verkkokalvon adaptaatiotila eli adaptaatioluminanssi määritellään.

Tässä työssä analysoitiin adaptaatioluminanssia valaistussa tieympäristössä. Työssä mitattiin koehenkilöiden kontrastikynnystä luminanssijakaumaltaan epäyhtenäisissä näkökentissä, arvioitiin estohäikäisyn vaikutusta adaptaatioluminanssiin, ja suunniteltiin järjestelmä, joka yhdistää kuvantavan luminanssimittauksen laserskannattuun 3D-pistepilveen.

Luminanssijakauman epäyhtenäisyys heikensi selvästi näkötehtävien suorittamista. Vaadittu kontrastikynnys saattoi epäyhtenäisellä taustalla olla kaksinkertainen verrattuna yhtenäiseen taustaan. Lisäksi tulokset viittasivat, että eri verkkokalvon alueet sopeutuisivat itsenäisesti omaan paikalliseen adaptaatioluminanssiinsa.

Katuvalaistusmittauksissa harsoluminanssi nosti adaptaatioluminanssia keskimäärin 29 prosentilla. Harsoluminanssi nostaa adaptaatioluminanssia siirtäen verkkokalvon spektriherkkyyttä kohti fotooppista näkemistä. Tästä mesoopisen luminanssin laskemiseen aiheutuva ero oli keskimäärin |0.6%|.

Havannoijan pituussuuntainen sijainti tiellä vaikuttaa adaptaatioluminanssiin ja mitattavan alueen mesooppiseen luminanssiin. Pituussuuntaisesta sijainnista johtuva suhteellinen keskihajonta oli 4,4 % lasketuissa mesoopisissa luminasseissa.

Mitattujen luminanssiarvojen yhdistäminen laserskannattuun pistepilveen onnistui lupaavasti.

Adaptaatioluminanssin määrittelemiseksi tarvitaan lisää tutkimusta. Tällä hetkellä yhdelläkään harsoluminanssimallilla ei voi riittävällä tarkkuudella laskea harsoluminanssia mielivaltaiselle verkkokalvon pisteeseelle. Lisäksi jatkuvasti muuttuvan näkemisympäristön vaikutus adaptaatioon pitäisi määrittää. Kolmanneksi näkötehtävän fysiologinen ja kognitiivinen osa olisi eroteltava. Kuitenkin käytännön tievalaistuslaskennassa mittausalueen luminanssi voi usein olla riittävä arvio adaptaatioluminanssiksi.

Avainsanat adaptaatioluminanssi, mesooppinen fotometria, tievalaistus, estohäikäisy

ISBN (painettu) 978-952-60-6988-3 **ISBN (pdf)** 978-952-60-6987-6

ISSN-L 1799-4934 **ISSN (painettu)** 1799-4934 **ISSN (pdf)** 1799-4942

Julkaisupaikka Helsinki **Painopaikka** Helsinki **Vuosi** 2016

Sivumäärä 133 **urn** http://urn.fi/URN:ISBN:978-952-60-6987-6

Preface

The research work of this thesis was conducted in the Lighting Unit of Aalto University School of Electrical Engineering. The work was funded by Aalto Energy Efficiency research programme, the research project being Light Energy – Efficient and Safe Traffic Environments.
I am utterly grateful to my supervisor Professor Liisa Halonen for her trust on me from the very first day she recruited me to work in the Lighting Unit.
I am extremely thankful to my instructors Marjukka Puolakka for her outstanding accuracy for details – the skill I often lack, and Eino Tetri for his supportive and encouraging colleagueship.
I would like to thank the preliminary examiners Professor Yandan Lin and Professor Miyoshi Ayama for their detailed observations and comments on this thesis. I am thankful to Professor Stephan Völker for opposing me in the defense of this thesis.
I would like to thank Can Cengiz for his leading contribution in publications I and II, and Esko Aalto for his invaluable work making the publications I and II possible.
I am grateful for my colleagues Matti Vaaja, Matti Kurkela, Juho-Pekka Virtanen, Hannu Hyyppä, and Juho Hyyppä for the cooperation in publication V.
I am thankful for each and every colleague and staff member I worked with in Aalto University for creating a truly peaceful and helpful working environment.
I would like to thank my family and kin, and my friends - ur awsum ftw. And of course, I most preferably am grateful to my dear waifu Mari.

Maari, August 2016
Mikko Maksimainen

List of Publications

This doctoral dissertation consists of a summary and of the following publications, which are referred to in the text by their numerals

I Cengiz, Can; Maksimainen, Mikko; Puolakka, Marjukka; Halonen, Liisa. Contrast threshold measurements of peripheral targets in night-time driving images. Lighting Research and Technology, vol. 48, no. 4, pp. 491-501, June 2016.

II Cengiz, Can; Maksimainen, Mikko; Puolakka, Marjukka; Halonen, Liisa. Effects of high luminance objects on peripheral target detection in night-time driving images. Light and Engineering, vol. 24, no. 1, pp. 12-20, March 2016.

III Maksimainen, Mikko; Puolakka, Marjukka; Tetri, Eino; Halonen, Liisa. Veiling luminance and visual adaptation field in mesopic photometry. Accepted for publication in Lighting Research and Technology on February 13th 2016. Published online on March 23rd 2016.

IV Maksimainen, Mikko; Puolakka, Marjukka; Tetri, Eino; Halonen, Liisa. Observer's longitudinal road location in mesopic photometry. Submitted to Light and Engineering on April 4th 2016.

V Vaaja, Matti; Kurkela, Matti; Virtanen, Juho-Pekka; Maksimainen, Mikko; Hyyppä, Hannu; Hyyppä, Juho; Tetri, Eino.Luminance-Corrected 3D Point clouds for road and street environments. Remote Sensing, 2015, 7(9), 11389-11402; DOI:10.3390/rs70911389.

The author played a major role at each stage of the work presented in this thesis. The author participated in the measurements, the initial design, and creating the novel experiment methods in publications I and II. The author took responsibility as the main author in publications III and IV. As the main author, the author gathered the data, conducted the measurements, and analysed the data. In publication V, the author participated in the initial design, measurements, and development of the experiment methods.

Contents

List of Abbreviations and Symbols

Abbreviations

2D	two-dimensional
3D	three-dimensional
AOM	area of measurement – the measurement field
CEN	European Committee for Standardization
CIE	Commission Internationale de l'Eclairage
CT	contrast threshold – the smallest detectable contrast
HPS	high pressure sodium
IES	Illumination Engineering Society
ISO	International Organization for Standardization
LED	light emitting diode
TLS	terrestrial laser scanning

Symbols

E	illuminance [lx]
E_{gl}	illuminance to a vertical plane at the observer's eye [lx]
E_{per}	illuminance to a plane perpendicular to a straight line between observer's eye and the light source [lx]
L	luminance [cdm^{-2}]
L_{ave}	average luminance [cdm^{-2}]
$L_{ave,road}$	average luminance of the road surface [cdm^{-2}]
L_b	background luminance [cdm^{-2}]
L_{mes}	mesopic luminance [cdm^{-2}]
$L_{mes,true}$	mesopic luminance calculated with taking into account the luminous efficiency shift caused by veiling luminance [cdm^{-2}]
L_t	target luminance [cdm^{-2}]
L_{veil}	veiling luminance [cdm^{-2}]
S/P ratio	scotopic to photopic ratio
$V(\lambda)$	CIE photopic spectral luminous efficiency function
$V'(\lambda)$	CIE scotopic spectral luminous efficiency function
$V_{\mathrm{mes}}(\lambda)$	CIE mesopic spectral luminous efficiency function

1. Introduction

1.1 Background

Mesopic photometry emerged from the need to improve the measurement accuracy in the luminance region, where both the rod and the cone cells contribute to vision. The reflective surfaces in outdoor lighting scenery, especially in the road lighting environment, are often in the mesopic luminance region. Using mesopic photometry, we would be able to optimise the visibility conditions of road lighting [1]. Hence, utilising mesopic photometry, instead of photopic photometry, would have two societal impacts: improvement of traffic safety and reduction of energy consumption.

In mesopic photometry, neither the scotopic $V'(\lambda)$ nor the photopic $V(\lambda)$ spectral luminous efficiency function solely applies. Instead, the spectral distribution of the luminaire and the adaptation state of the retina determine the mesopic spectral luminous efficiency function $V_{mes}(\lambda)$. The mesopic luminance region was defined as 0.005 cd/m² – 5 cd/m² by CIE (Commission Internationale de l'Eclairage) in 2010 [2]. The CIE 191 visual performance-based system for mesopic photometry defines $V_{\mathrm{mes}}(\lambda)$ as follows:

$$M(m)V_{mes}(\lambda) = mV(\lambda) + (1-m)V'(\lambda)$$

$$L_{mes} = \frac{683}{V_{mes}(\lambda_0)} \int V_{mes(\lambda)L_e(\lambda)d\lambda} \qquad (1)$$

where m is a coefficient, the value of which depends on the adaptation; $M(m)$ is a normalising function, such that $V_{mes}(\lambda)$ attains a maximum value of 1; $V_{mes}(\lambda_0)$ is the value of $V_{mes}(\lambda)$ at 555 nm; L_{mes} is the mesopic luminance; $L_e(\lambda)$ is the spectral radiance in $\mathrm{Wm^{-2}sr^{-1}}$; if $L_{mes} \geq 5$ $\mathrm{cdm^{-2}}$, then $m = 1$; if $L_{mes} \leq 0.005$ $\mathrm{cdm^{-2}}$, then $m = 0$. The coefficient m and the mesopic luminance L_{mes} can be calculated using an iterative approach as follows:

$$m_0 = 0.5\,,$$

$$L_{mes,n} = \frac{m_{(n-1)}L_p + (1-m_{(n-1)})L_s V'(\lambda_0)}{m_{(n-1)} + (1-m_{(n-1)})V'(\lambda_0)},$$

$$m_n = a + b \log_{10}(L_{mes,n}/L_0) \qquad \text{for } 0 \leq m_n \leq 1, \qquad (2)$$

Where L_p is the photopic luminance of the visual adaptation field; L_s is the scotopic luminance of the visual adaptation field; $L_0 = 1$ cdm^{-2}; and $V'(\lambda_0) = 683 / 1699$ is the value of scotopic spectral luminous efficiency function at $\lambda_0 = 555$ nm; a and b are parameters which have the values $a = 0.7670$ and $b = 0.3334$; and n is the iteration step. [2]

The photopic luminance of the visual adaptation field can be considered as the adaptation luminance, the luminance representing the adaptation state of the retina. However, neither 'the visual adaptation field' nor 'the adaptation luminance' has a final definition. In addition, disability glare sources cause veiling luminance, which increases the adaptation luminance. Currently, the interaction between veiling luminance and adaptation luminance is not completely clarified or quantified for road lighting conditions.

In a visual field with a completely uniform luminance distribution, the adaptation luminance is naturally the same as the luminance of the visual field. In practice, the luminance distribution of a road lighting visual environment is never completely uniform. The relation between a luminously non-uniform visual field and the adaptation luminance lacks definition. To define the adaptation luminance, analysis on the luminance distribution features of the visual environment, especially the disability glare sources, is needed.

1.2 Aim of the study

The aim of this work is to analyse the adaptation luminance in street and road lighting environments. A definition for adaptation luminance is needed in order to implement the CIE 191:2010 system for mesopic photometry [2]. The focus is particularly on quantifying the increment or the decrement in the adaptation luminance, caused by luminance differences in the visual field. This is realised by examining the test subjects' contrast thresholds within visual fields, where the luminance distributions were non-uniform. Disability glare sources are the extreme instances of luminance non-uniformity. Their influence on the adaptation luminance is quantified by street environment luminance measurements and disability glare calculations.

2. State of the art

2.1 Mesopic photometry

The retinal photoreceptor cells are the foundation of our visual system [3]. There are two main types of photoreceptors: cones and rods [4]. Cone cells enable our photopic vision (daylight vision), and the photopic spectral luminous efficiency function was defined in 1924 [5, 6]. Rod cells enable our scotopic vision (dark vision), and the scotopic spectral luminous efficiency function was defined in 1951 [7, 8].

The luminance region, in which both the cones and the rods contribute to vision, is called the mesopic region [9]. Hence, in the mesopic region, neither the scotopic nor the photopic spectral luminous efficiency function solely is fully compatible. Moreover, the mesopic luminous efficiency depends on the light levels in the visual environment, as the light levels determine the interaction between rods and cones. Therefore, a need emerged to define the mesopic photometry.

An early suggestion for a system for mesopic photometry was proposed by Palmer in 1966 [10]. The system was based on brightness matching, an experimental method where the test subject adjusts the brightness of a stimulus with a certain spectral power distribution to match the brightness of a reference white surface. This approach was further examined, and the mesopic spectral luminous efficiency was found to be dependent on the retinal illuminance. It was also found that the mesopic spectral luminous efficiency could not be represented by a single function [11, 12]. However, the brightness-matching approach suffers from additivity failure, in which the luminance of a light source does not correspond to a weighted integration of radiance over the spectral domain [13].

Due to the inherent problem of brightness matching, an approach that was based on visual task performance was found more promising in several studies [14-16]. The combined effort in studying the visual task performance approach culminated in the CIE 191:2010 system for mesopic photometry [2]. In 191:2010, the mesopic range was defined as the luminances between 0.005 and 5 cd/m^2. Using the system, we can calculate the mesopic luminance, when the photopic adaptation luminance and the S/P–ratio of the light source are known. However, the CIE 191:2010 system for mesopic photometry is not fully

implementable until we can reliably determine the adaptation luminance in the retina.

2.2 Adaptation luminance

Adaptation is a neural and a photochemical process, in which the retina adjusts to the quantity of light in the visual environment [17, 18]. Adaptation luminance is the luminance value associated with the adaptation state, which is the completion of the adaptation process [19]. In order to calculate the mesopic luminance, adaptation luminance is needed, as it determines the spectral sensitivity in the retina [20, 21].

In a uniform visual field, the adaptation luminance is obviously the luminance of the visual field. In a non-uniform visual field, the determination of adaptation luminance is complex, and even disputed. Adaptation can be considered mainly as a local phenomenon, where different retinal locations adapt independently [22]. In contrast, adaptation in a given retinal location is also considered to be affected by the luminance features in a non-corresponding area of the visual scene [2]. In addition, rods and cones are unevenly distributed on the retina, and the *absolute* sensitivity of a photoreceptor depends on its retinal location [23]. Furthermore, also the *spectral* sensitivity depends on the retinal location, but mainly as a result of the discrimination between the fovea and the periphery, and less when two peripheral locations are compared [24].

High-luminance objects (disability glare sources) cause intraocular stray light [25]. This phenomenon is known as veiling luminance, as the scattered light adds veiling luminance on the retina and increases the adaptation state [26]. Hence, in order to quantify the adaptation luminance, the veiling effect of intraocular stray light should be quantified.

Currently, the CIE work group JTC-1 works to define how to determine the adaptation luminance. In JTC-1, several factors that contribute to the state of adaptation are considered. These factors include the luminance distribution of the visual environment, the veiling luminance, eye movements and the temporal characteristics of adaptation. This thesis contributes directly to the knowledge on the effect of the luminance distribution and the veiling luminance. The effect of luminance distribution is analysed by comparing visual performance in situations where luminance distribution is uniform to visual performance, in situations where luminance distribution is non-uniform. Furthermore, the retinal localness of adaptation is further elaborated. Veiling luminances are calculated for several road lighting environments. This statistical data contributes directly for JTC-1 analyses.

Another CIE work group, TC 2-65, defines how to practically apply adaptation luminance to calculate the mesopic enchantment factor for the luminous flux

of a luminaire. In this thesis, a method is used, where the mesopic luminance of the measurement area can be approximated using the measured photopic luminance and the estimated adaptation luminance. This method provides similar results for mesopic luminance, as the mesopic enchantment factor - method described in CIE ED/TN TC-2-65(2).

2.3 Veiling luminance

The first mathematical model to calculate the veiling effect of a peripheral high luminance source was developed in 1926 by Holladay [27]. The original equation (Equation 3) is:

$$B_1 = 4.3 \sum \frac{E}{D^2} \quad (3)$$

where B_1 is the veiling luminance in millilamberts, E is the unidirectional illuminance at the observer eye from the high-luminance source, and D is the angle in degrees between the observer's line of vision and the high-luminance source [27]. This equation has since been revised and improved several times, for example by Stiles [28], Crawford [29], Fry [30], Adrian and Vos [31]. In 2002, CIE published an equation (Equation 4), in which the continuum of veiling luminance research was compiled [32]:

$$L_{veil} = E_{gl}\{\frac{10}{\theta^3} + \left[\frac{5}{\theta^2} + \frac{0.1p}{\theta}\right] * [1 + (\frac{A}{62.5})^4] + 0.0025p\} \quad (4)$$

where L_{veil} is the veiling luminance caused by a high-luminance light source; θ is the angle (in degrees) between the line of fixation and the high-luminance source; A is the observer's age in years; p is the eye pigmentation factor; and E_{gl} is the illuminance to a vertical plane at the observer's eye.

The model for calculating the veiling luminance in foveal vision is well studied. However, calculating the veiling effect for peripheral vision is not considered in the veiling luminance models mentioned above. A veiling luminance model was extended to be applicable for peripheral vision in a study by Uchida and Ohno [33]. Their equation (Equation 5) is as follows:

$$L_{veil} = E_{per} \frac{260}{\theta^3} \quad (5)$$

where E_{per} is the illuminance at a plane perpendicular to a straight line between the observer's eye and the light source, and θ is the angle (in degrees) between the high-luminance source and the task point. However, the study also states that the equation may not be accurate when the angle, θ, is smaller than 7°.

In recent studies, a spectral dependency for intra-ocular stray light has been confirmed. The amount of stray light was found highest for red light (>630 nm) and lowest for green light (~550 nm) [34, 35]. The spectral dependency of

veiling luminance should be considered in mesopic photometry, as mesopic photometry itself is relative to the spectrum of the light source. In this thesis, veiling luminance caused by reddish high-pressure sodium light is compared to veiling luminance caused by bluish LED light. However, the experimental setup does not enable an accurate comparison, and the spectral dependency of veiling luminance in a road lighting environment was left unconsidered.

To define mesopic photometry, we first need to define both the foveal and the peripheral adaptation luminance. To define peripheral adaptation luminance, we first need to be able to calculate peripheral veiling luminance reliably and accurately. However, none of the existing veiling luminance models are fully capable of being utilised for an arbitrary retinal coordinate. In addition, we need to determine the adaptation-impact of a luminance non-uniformity that is not bright enough to cause veiling luminance per se, yet distracts the visual task performance.

3. Contrast threshold in simulated road lighting conditions

3.1 Introduction

Contrast threshold (CT) and visual sensitivity experiments have been used to estimate the visual adaptation in several studies involving mesopic photometry and adaptation luminance [36-39]. Two laboratory experiments (Publications I & II) were conducted in order to study the observer's contrast threshold in simulated road lighting conditions. The contrast thresholds were examined with 1.5° circular targets, presented both in test subjects' foveal and peripheral vision. The night-time road lighting scenery provided various encompassing backgrounds for the targets, in terms of luminance level and luminance distribution uniformity.

The road lighting scenery used in these two studies (I & II) was found suitable for trialling the local adaptation hypothesis [22]. In the local adaptation approach, adaptation is not considered as a global phenomenon on the retina, where only one adaptation luminance value would be applied to every retinal location. Instead, different parts of the retina are considered to be adapted to a local adaptation luminance value independently. Confirming whether adaptation is a local or a global phenomenon on the retina would be a step forward in the definition of adaptation luminance.

3.2 Methods

In the laboratory setting, the visual scenery was projected to a cylindrical screen using three BenQ W1070 projectors. The test subjects sat at a distance of 96 cm from the screen (Figure 1). From the subject's point of view, the screen covered the visual field 44° vertically and 180° horizontally.

Figure 1. The test subject's position to the cylindrical screen.

Both of the experiments included ten subjects with a mean age of 30 years. The subjects were confirmed to have normal colour visions, using the Ishihara colour vision test. The experimental session began with a 5-minute adaptation period, during which the background was presented without any targets. The subjects were given a control device and were asked to press the button on the device as they detected a target in their visual field. During the experiment, the test subjects were instructed to fixate on a faint cross in the centre point of the cylindrical projection screen. The test subjects' eye fixations were monitored via camera by the experiment supervisor.

The experiment was controlled using a purpose-built Labview programme. The programme placed the 1.5° circular targets to the target locations. The targets appeared slowly, with their luminance gradually doubling over the time period of 10 seconds. The test subject pressed the button at the time of target detection, and the contrast threshold was determined from the target's luminance at this moment. If the test subject could not perceive the target during this time period, the target disappeared at that location, and a new target was introduced at a new location. The gamma function of the projectors was inverted using an inverse gamma function in the Labview programme to make the target's luminance appearance linear in terms of increased luminance per second.

The visual scenery used in these two experiments was an image taken at Otaranta (Figure 2), a quiet suburban street in Espoo, Finland. The lighting class of Otaranta was AL4b, which is, apart from the longitudinal uniformity, similar to the class ME4b in the CEN 13201-1 standard. The image was taken using a Canon 60D digital camera mounted with an 8 mm lens objective. The camera was placed in front of the car, in between the headlights, at the height of 1.5 metres. Both the street luminaires (AEC Illuminazione LEDin 54 LED-luminaires (90 W, 4000 K)) and the car headlights illuminated the scene. The

spectrum of the real scene per se, was not a governing factor, as the final spectrum was generated by the RGB projectors. In the projection, the measured S/P –ratio of the screen radiance was 2.02.

Figure 2. Otaranta in Espoo, Finland. The visual scene used in the contrast threshold experiments.

3.2.1 Contrast thresholds in the road lighting visual scene

In both of the contrast threshold experiments, two background luminance levels were used for the same visual scene. These two levels are referred to as 'high luminance' and 'low luminance' scenes. In the experiments, the luminance level was controlled using neutral density filters (0.6 and 0.9) on the projectors' lenses.

In the first experiment, the average luminance of the projected screen for the 'low luminance' was 0.34 cd/m², and for the 'high luminance' 0.76 cd/m². The real average luminance measured at the same point in Otaranta was 0.46 cd/m². The highest luminances found in the projected visual scenes were located at the luminaires and were 19 cd/m² and 37 cd/m² in 'low luminance' and 'high luminance' scenes respectively. Creating a realistic dynamic range of the luminances was not possible in this experimental set-up. Thus, the maximum luminances of the projected visual scene did not represent the real luminance values of the luminaires (10000 cd/m² - 20000 cd/m²) at Otaranta. The luminances were measured using an LMK Mobile Advanced imaging luminance photometer and an LMT 1009 spot luminance meter.

In the first experiment, the 1.5° circular targets were presented at 23 target locations (Figure 3). Locations 1, 2, 3, 4, 7, 12, 17, 20, 21, 22, and 23 represent the horizontal axis for eccentricities -60°,-45°,-30°,-20°,-10°,0°, 10°,20°,30°,45°, and 60° respectively. Target 12 was the fixation point. Target locations 8, 9, 11, 13, 15, and 16 represent the 10° circular eccentricity from the fixation point, and locations 5, 6, 10, 14, 18, and 19 the 20° circular eccentricity from the fixation point. The time interval between the target appearances was randomized between 500 ms and 2000 ms. In addition, the order of appearance of the target locations was also randomized.

Figure 3. The visual scene and the target locations of the first experiment.

For each target location, the average luminance of the encompassing surrounding area, 3° circular field, was measured. This value was used as the background luminance, L_b, to calculate the contrast threshold, CT as follows:

$$CT = \frac{|(L_b - L_t)|}{L_b} \quad (6)$$

where L_t is the final target luminance, at the moment of detection. In addition, a factor named 'Complexity' was coined to represent the local luminance non-uniformity around the target location:

$$Complexity = 1 - \frac{L_{min}}{L_{ave}} \quad (7)$$

where L_{ave} is the average luminance of a 5° circular field surrounding the target, and L_{min} the minimum luminance value within that field.

3.2.2 Contrast threshold in a visual scene with reduced non-uniformity

In terms of experimental set-up, the second contrast threshold measurement was identical to the first one, apart from a few important details. Firstly, there were two additional peripheral target locations on the horizontal axis: -75° and 75° from the fixation point. Due to the addition of these two targets, targets 1, 2, 3, 4, 5, 8, 13, 18, 21, 22, 23, 24, and 25 represent the horizontal axis; 9, 10, 12, 16, and 17 represent the circular field of 10°; and 6, 7, 11, 15, 19, and 20 represent the circular field of 20°. Secondly, and more importantly, two different versions of the visual scene were presented to the test subjects. The first version was identical to the visual scene used in the first experiment. In the second version, the street luminaires and the luminaires of the background scenery were obstructed from the visual scene. Consequently, the overall non-uniformity of the luminance distribution was reduced. Figure 4 presents the original visual scene, and Figure 5 the scene with the reduced non-uniformity.

Figure 4. The visual scene and the target locations for the second experiment. Original luminance distribution.

Figure 5. The visual scene and the target locations for the second experiment. Luminance distribution with reduced non-uniformity.

3.3 Results

3.3.1 Correlation between contrast threshold and complexity

The contrast threshold data were statistically analysed in terms of target background complexity and target location. The Pearson product moment correlation coefficient [40] was utilised to measure the linear correlation between the elements: contrast threshold – complexity; contrast threshold – target location.

Figure 6 and Figure 7 present the contrast thresholds, complexity values, and the background luminances for the targets at the horizontal axis (1, 2, 3, 4, 7, 12, 17, 20, 21, 22, and 23) in the first experiment (Publication I). Figure 8 and Figure 9 present contrast thresholds, complexity values, and the background luminances for the targets on the 10° and 20° circular fields around the fixation point. The values are fully presented in Table 10 and Table 11 in the Appendices. The average difference, when comparing the contrast threshold of a target in a 'high luminance' scene and in a 'low luminance' scene were small, 11.6% on average. The targets in the extreme periphery were often missed by the test subjects. In the 'low luminance' scene, the miss percentages for targets at eccentricities -60° and 60° were 48% and 96% respectively. In the 'high luminance' scene, the corresponding percentages were 88% and 96%. There was no positive correlation found when comparing the contrast threshold values in the horizontal axis targets in pairs with corresponding eccentricity (-45° to 45°, -30° to 30°, -20° to 20°, and -10° to 10°). The Pearson correlation factors for the eccentricity pairs were -0.54 and 0.09 for 'low luminance' and 'high luminance' respectively. This was most probably a result of non-symmetricity of the visual scenery. The right-hand side was represented by the park, which was mostly a uniformly dark area, and the luminance distribution of the left-hand side was significantly more complex. The average complexities of the left- and right-hand sides were 0.49 and 0.23 respectively.

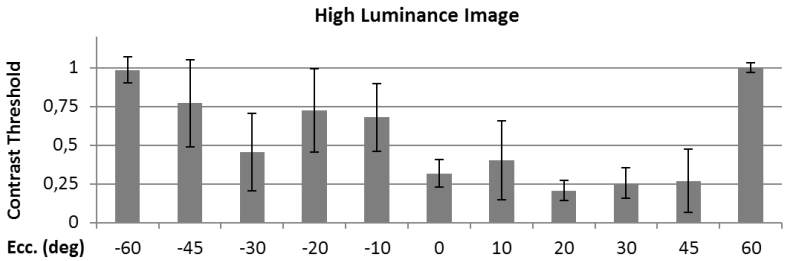

Complexity	0.68	0.31	0.36	0.60	0.70	0.73	0.36	0.22	0.08	0.26	0.15
Lum (cd/m^2)	0.22	0.27	0.20	0.66	0.61	0.39	0.28	0.21	0.16	0.20	0.23

Figure 6. The eccentricities, the contrast thresholds, the contrast threshold standard deviations (error bars), complexity values, and the background luminances for the targets on the horizontal axis (1, 2, 3, 4, 7, 12, 17, 20, 21, 22, and 23) in the first experiment ('high luminance').

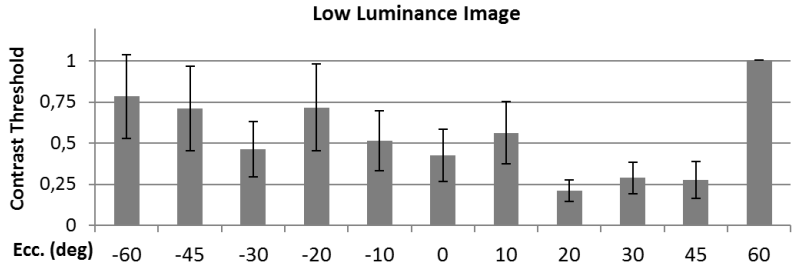

Complexity	0.65	0.30	0.39	0.58	0.71	0.75	0.38	0.25	0.10	0.10	0.16
Lum (cd/m^2)	0.10	0.12	0.09	0.28	0.26	0.14	0.11	0.08	0.07	0.09	0.10

Figure 7. The eccentricities, the contrast thresholds, the contrast threshold standard deviations (error bars), complexity values, and the background luminances for the targets on the horizontal axis (1, 2, 3, 4, 7, 12, 17, 20, 21, 22, and 23) in the first experiment ('low luminance').

a.)

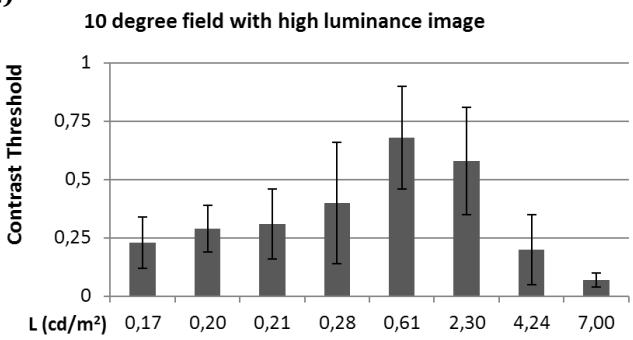

Complexity	0.49	0.38	0.87	0.36	0.70	0.91	0.81	0.76
Target no.	16	9	13	17	7	15	8	11

b.)

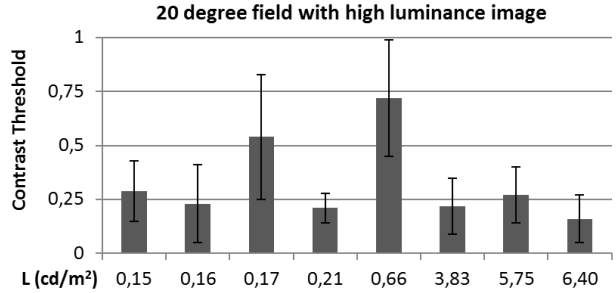

Complexity	0.11	0.21	0.95	0.22	0.60	0.44	0.77	0.86
Target no.	6	19	14	20	4	5	18	10

Figure 8. The eccentricities of the targets, the contrast thresholds, the contrast threshold standard deviations (error bars), the target background luminances, and the complexity values, for the numbered targets on the a.) 10° field and b.) 20° field in the first experiment ('high luminance').

a.)

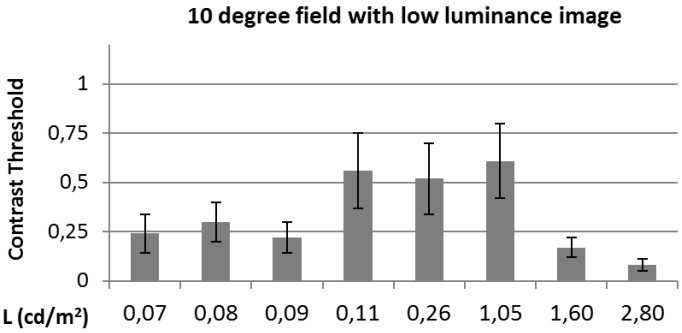

Complexity	0.50	0.32	0.86	0.38	0.71	0.92	0.83	0.70
Target no.	16	9	13	17	7	15	8	11

b.)

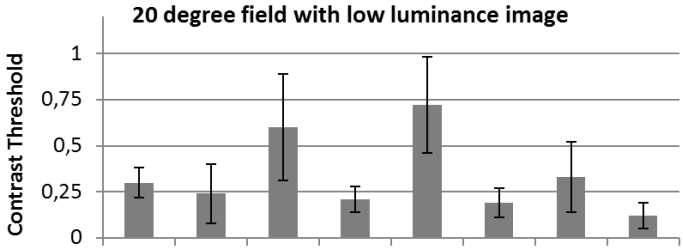

Complexity	0.13	0.25	0.92	0.25	0.58	0.47	0.76	0.59
Target no.	6	19	14	20	4	5	18	10

Figure 9. The eccentricities of the targets, the contrast thresholds, the contrast threshold standard deviations (error bars), the target background luminances, and the complexity values, for the numbered targets on the a.) 10° field and b.) 20° field in the first experiment ('low luminance').

Instead, higher complexity in the target's encompassing surroundings (5°) had a positive correlation with higher contrast threshold. In other words, the more luminously non-uniform was the target's encompassing area, the more difficult was the target detection. For the targets on the horizontal axis (excluding -60° and 60°), the Pearson correlation factors between the contrast thresholds and the complexity values were 0.48 and 0.43 for 'low luminance' and 'high luminance' scenes respectively. For all of the targets (excluding -60° and 60° on the horizontal axis), the corresponding correlation factors were only 0.14 and 0.11. Nevertheless, the complexity or the non-uniformity had stronger positive correlation with the contrast threshold than, for example, eccentricity. For certain targets, (14 and 15) in 'high luminance' for example, the correlation between the complexity value and the contrast threshold was very clear. On the other hand, the targets with the highest contrast threshold in 'high luminance' (excluding 1 and 23), targets 4 and 7, were not the targets with the highest complexity. The reason for this could be that the small, bright spots around targets 4 and 7 did not increase the complexity value by much,

but were very distractive for the peripheral target detection task. Thus, the way the complexity value is calculated may have underrated the distractive effect concerning these targets.

3.3.2 Local adaptation

When state of adaptation is reached, contrast sensitivity is optimal for the adaptation luminance, and is higher for luminances higher or lower than the adaptation luminance [41]. In the mesopic range, *CT* can be approximated from the background luminance, L_b, using the de-Vries-Rose law, assuming the retina is adapted to the L_b [42]. Evidence found in this study supports the local adaptation hypothesis. For example, targets 5 and 6 were both in 20° eccentricity from the centre. The visual angle between targets 5 and 6 was 28°. In the 'high luminance' scene, the background luminances for targets 5 and 6 were 3.83 cd/m² and 0.15 cd/m² respectively. Thus, the background luminance for target 5 was 2450% higher than the background luminance for target 6. However, the contrast thresholds for targets 5 and 6 were 0.19 (19%) and 0.30 (30%) respectively. Target 6 was detected, when the absolute luminance of the target was increased by 0.045 cd/m² compared to the background luminance, 0.15 cd/m². This increment, 0.045 cd/m², was 1.2% of the luminance surrounding target 5, 0.12% of the maximum luminance of the visual field (37 cd/m²), and 5.9% of the average luminance of the whole visual field (0.76 cd/m²). If the retina was globally adapted to the average luminance of the visual field, the estimated luminance increment needed for detection using the de-Vries-Rose law would have been 0.21 cd/m² [42]. This absolute luminance would mean a contrast threshold of 1.39 (139%) for target 6. Furthermore, if the retina was adapted to the L_b of target 5, the *CT* needed for the detection of target 6 would have been 4.8 (480%). Yet, the *CT* for target 6 was 0.30 (30%), nearly the same as for target 5 (0.19). The contrast threshold for both of the targets followed approximately the de-Vries-Rose law [42]. Similar local luminance behaviour was evident also for the target pairs: 6 & 18, 5 & 19, 18 & 19, 6 & 10, 19 & 10, 5 & 20, 8 & 13, and 11 & 13.

It is reasonable to suggest, that the part of the retina where, for example, target 6 was located, was adapted close to that value (0.15 cd/m²), and the part of the retina where target 5 is located, was adapted close to that value (3.83 cd/m²). To verify this, more research is needed. Especially, the dynamic range of the visual field was too small in this study to confirm the local adaptation approach. Yet, nothing in this study indicates that the adaptation would be a global phenomenon, where a single luminance value could represent the adaptation state for the whole retina.

3.3.3 The visual scene with the high luminance features removed

The second contrast threshold experiment (Publication II) featured a modified version of the visual scene in the first experiment. As shown in Figures 4 and 5, the original scene was compared to a visual scene in which the high luminance features were removed. The second experiment was also executed at two luminance levels: 'low luminance' and 'high luminance'. The average luminance of the modified visual scene was 0.27 cd/m² (down 21% from 0.34 cd/m² in the original scene) for 'low luminance', and 0.57 cd/m² (down 25% from 0.76 cd/m² in the original scene) for 'high luminance'. The maximum luminance of the modified visual scene was 6.9 cd/m² (down 64% from 19 cd/m² in the original scene) for 'low luminance', and 17 cd/m² (down 54% from 37 cd/m² in the original scene) for 'high luminance'. Figure 10 and Figure 11 show the measured contrast thresholds for the targets on the horizontal axis, and the measured values of the second experiment are presented in Table 12 and Table 13 in the Appendices.

The removal of the high luminance features reduced the contrast threshold in both low luminance and high luminance scenes, and for almost every target. The percentage of missed targets was halved from 18.3% to 9.3% in the 'low luminance' scene, and cut to one-third from 22.9% to 7.7% in the 'high luminance' scene. The average contrast threshold was reduced from 0.46 to 0.36 in both scenes. In few exceptional targets though, for example target 8 in 'low luminance', the contrast threshold increased in the modified scene. No clear reason for this was found. The detection of far peripheral targets improved more, than the detection of the targets closer to the foveal vision.

The calculated veiling luminance caused by the luminaires in the original scene was small, 0.01 cd/m² for the 'high luminance', and 0.005 cd/m² for the 'low luminance'. Removing this neglectably small veiling effect cannot explain the reduction in contrast thresholds. In other words, the lowered visual performance in the simulation, where the luminaires existed in the scene, was not caused by veiling luminance but by another mechanism. The high luminance objects in the near periphery seem either to increase the adaptation luminance in the far periphery or distract the target detection via a cognitive mechanism. It is difficult to distinguish between these two mechanisms, adaptation state and cognition, as they function simultaneously.

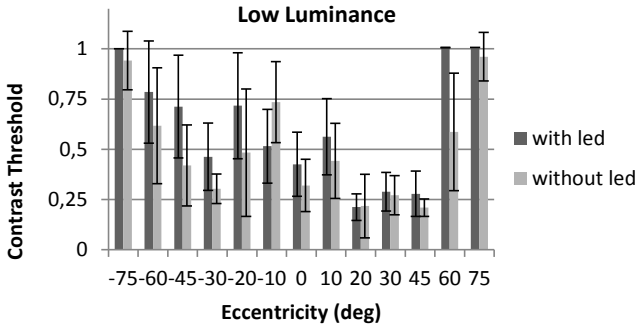

Figure 10. The contrast thresholds for the targets on the horizontal axis in the 'low luminance' visual scene. The bars 'with led' indicate the contrast thresholds in the original scene, and the bars 'without led' indicate the contrast thresholds for the scene where the higher luminance sources were removed.

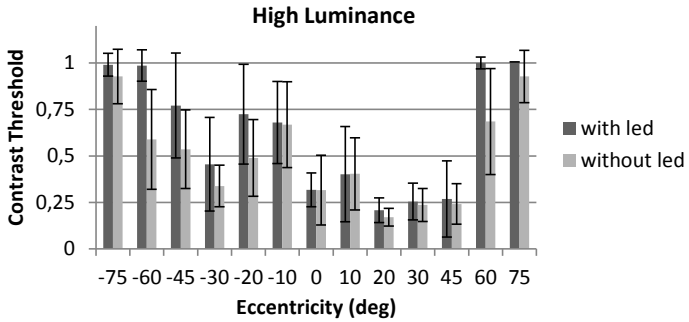

Figure 11. The contrast thresholds for the targets on the horizontal axis in the 'high luminance' visual scene. The bars 'with led' indicate the contrast thresholds in the original scene, and the bars 'without led' indicate the contrast thresholds for the scene where the higher luminance sources were removed

3.4 Summary

Two experiments were conducted to study contrast thresholds in a simulated road lighting visual environment. In these experiments, test subjects were presented with a visual scene of a night-time road, and targets with gradually increasing luminance. The contrast between the target (1.5° circular field) and its surrounding background (3° circular field) at the moment of target detection was considered as the contrast threshold. A factor named 'complexity' presented the non-uniformity in a 5° circular area encompassing the target location. The first experiment focused on the effect of this non-uniformity and the average luminance in the target location, and also the target's eccentricity from the fixation point. In the second experiment, the non-uniformity of the whole visual scene was reduced by removing the high luminance features of the scene image, and the effect of this was analysed. Both experiments were executed using two luminance levels: the 'low luminance' and the 'high luminance' scenes.

In the first experiment, there was no significant difference in the contrast thresholds between the 'low luminance' and the 'high luminance' scenes. Furthermore, the eccentricity from the fixation point did not matter in terms of the contrast threshold if the most peripheral targets (-60° and 60°) were not considered. The higher background luminance in the target location reduced the contrast thresholds generally, but not for every visual target. Higher complexity in the target location correlated with higher contrast threshold. In other words, targets on a non-uniform background were generally harder to detect than targets on a uniform background.

On a low luminance background (0.15 cd/m^2), a small increment of 0.045 cd/m^2 was detectable for one target. This target was within a 28° visual angle from another target with background luminance of 3.83 cd/m^2. The detected increment for the first target was only 1.2% of the background luminance of the second target. Yet, the first target was detected with a contrast threshold of 0.30, which indicates that this retinal coordinate was adapted to the background luminance of the corresponding location in the visual field. Furthermore, the contrast threshold for the second target was also low: 0.19. This discovery suggests, that these two retinal locations were independently adapted to, and thus, supports the local adaptation luminance approach. Similar behaviour was evident in several target pairs.

Increasing the luminance uniformity of the whole visual field by removing the high luminance features improved the overall target detection and decreased the contrast thresholds. The average of missed targets was halved in the 'low luminance' scene and was cut to one-third in the 'high luminance' scene. The average contrast threshold was reduced by 22% in both of the scenes. It could not be clearly determined whether this detection improvement was caused by adaptation, cognition or both.

The experimental method used was successful for measuring the contrast thresholds in simulated road lighting scenes. However, the experimental setup was unable to represent realistic dynamic range of night-time traffic conditions. In order to study the effect of discomfort glare and disability glare, increasing the dynamic range in the experiment would be important, as both the discomfort glare [43] and the disability glare [44] affect the visual performance. Furthermore, movement and the flow of traffic were not simulated in these experiments. More research is needed, to study how the high dynamic range or the movement affect visibility. Furthermore, it is difficult to differentiate when visual performance is lowered by a cognitive process, and when by a non-optimal adaptation state. To study this, novel methods should be developed.

4. Veiling luminance and adaptation luminance in road lighting conditions

4.1 Introduction

The CIE 191:2010 system for mesopic photometry is not completely applicable without the definition of adaptation luminance. Adaptation luminance is considered to be the average luminance of a visual adaptation field, which has yet to be defined in terms of the size, shape or location within the visual field. Furthermore, the adaptation state of the retina is considered to be presented by the adaptation luminance. However, glare sources outside of the visual adaptation field can increase the adaptation state if they cause veiling luminance. Hence, the definition for adaptation luminance is contradictory when the visual field is non-uniform in terms of luminance distribution. Therefore, two studies were conducted in road lighting conditions, to analyse the possible variation in adaptation luminance caused by high-luminance sources and different choices for an adaptation field. In addition, a road-condition study was conducted to develop new methods to define the visual adaptation field.

The term 'area of measurement' or AOM stands for the measurement area. The luminances are measured only for the AOM part of the observer's visual field. In the currently used EN-13201 standard, the area of measurement is the road surface between two adjacent street luminaires, and the distance between the observer and the first street luminaire is 60 m [45]. For mesopic photometry, AOM is not defined. In Publications III and IV, the AOM and the adaptation field are considered the same area of the visual field. Furthermore, adaptation luminance, L_a, is considered the sum of the measured average photopic luminance of the adaptation field, L_p, and the calculated veiling luminance L_{veil} (Equation 8):

$$L_a = L_p + L_{veil} \tag{8}$$

The purpose of the first road lighting study (Publication III) was to quantify the adaptation luminances calculated using circular or elliptical adaptation fields of different sizes and the 'road surface' adaptation field. The second purpose of the first study was to determine the average increment to the adaptation state caused by veiling luminance. This was done in order to identify the

bias in mesopic photometry, if the mesopic calculation neglects the veiling luminance caused by high-luminance sources outside the adaptation field.

One of the main application areas for mesopic photometry is road lighting. Road lighting measurements are currently done from single observer location: 60 metres from a luminaire pole, in the middle of a lane, and at the height of 1.5 metres [45]. Currently, this method is considered to provide the necessary luminance information of the road surface in photopic photometry. However, in mesopic photometry, not only the road surface but also the adjacent areas determine the adaptation luminance. In addition, the adaptation state is influenced by the veiling luminance, which is location-dependent. Thirdly, traffic is usually a flow of movement along the road rather than stasis. Therefore, it is important to recognise the dependency between the observer's longitudinal location and the mesopic luminance. Therefore, the purpose of the second road lighting study (Publication IV) was to identify the variance in the mesopic luminances that originates from the observer's longitudinal location.

Novel methods could improve road lighting measurements and help define the visual adaptation field further. Mobile laser scanning can be utilised to create a 3D model of a road environment. The 3D model can be combined with luminance measurements to create a 3D model of luminance data. The 3D luminance model can be utilised, for example, to calculate the veiling luminance at any observer point, as the distances to the luminaires are known. The third road lighting study (Publication V) was conducted to develop a method, where mobile laser scanning was combined with luminance data.

4.2 Methods

4.2.1 The experimental setup in visual adaptation field, veiling luminance, and adaptation luminance study

Three veiling luminance models were used in the first road lighting study (Publication III): Fry (Equation 9) [29] ; CIE general disability glare equation (Equation 4) [32]; and Uchida and Ohno (Equation 5) [33].

$$L_{veil} = 9.2 \sum \frac{E_{gl}}{\theta(\theta+1.5)} \quad (9)$$

$$L_{veil} = E_{gl}\{\frac{10}{\theta^3} + \left[\frac{5}{\theta^2} + \frac{0.1p}{\theta}\right] * [1 + (\frac{A}{62.5})^4] + 0.0025p\} \quad (4)$$

$$L_{veil} = E_{per}\frac{260}{\theta^3} \quad (5)$$

where L_{veil} is the veiling luminance caused by a high-luminance light source; θ is the angle (in degrees) between the line of fixation and the high-luminance

source; and A is age in years; p is the eye pigmentation factor. E_{per} is the illuminance to a plane perpendicular to a straight line between the observer's eye and the light source. E_{gl} is the illuminance to a vertical plane at the observer's eye. Consequently, E_{gl} is E_{per} multiplied by the cosine of θ.

Equations 9, and 4 are fairly similar in their fundamental behaviour, and the theory behind them was introduced in Holladay's experiments on glare in 1926 [27]. Equation 4 is stated as a further elaboration of Equation 9, containing an age-adjustment and eye pigmentation factor [32]. Despite the similarity between these equations, it was still considered meaningful to calculate and compare their outputs.

In Equations 9 and 4, the veiling luminance is calculated for the eye fixation point at the centre of the fovea. Equation 5 is different, and was designed to provide the veiling luminance or 'the surrounding luminance effect' for any task point in the visual field correlating to any retinal coordinate. According to the local luminance hypothesis, adaptation is a local, rather than global, phenomenon on the retina [33]. Of the compared equations, only Equation 5 can be used to calculate the veiling luminance for every retinal location, and Equations 9 and 4 only for the special case of the fovea.

Three different road lighting situations were employed in the first study (Publication III). Case 1 was Otaranta, Espoo, a quiet two-lane street with no buildings on either side of it. The street luminaires in Case 1 were AEC Illuminazione LEDin 54 LED-luminaires (90 W, 4000 K). The luminaires were pole-mounted on the right-hand side from the observer's point of view. The mounting height was 10.3 metres. Cases 2 and 3 were at the location of Topeliuksenkatu, Helsinki, from north to south and from south to north, respectively. Topeliuksenkatu is a two-lane urban street lit by Idman P2-95 LDT high pressure sodium luminaires (250 W), and with apartment buildings on the eastern side and a park on the western side. Figure 12 illustrates Otaranta and Figure 13 illustrates Topeliuksenkatu. In Case 2, the first eight luminaire pairs from the observer's position were taken into account in the luminance calculations, and in Case 3, the first seven pairs. It was expected that the effect of the furthermost luminaires on the veiling luminance was negligible. When using Equation 5, only the first two luminaires were taken into account in Case 1. When using Equation 5, only the first three luminaire pairs were taken into account in Cases 2 and 3. This was because Equation 5 is not defined for angles smaller than 7°. The observer point was in the middle of the right hand lane at a height of 1.5 m. In Case 1, the observer point was at a 60-metre distance from the second-closest luminaire. In Cases 2 and 3, the observer point was at a distance of 60 m from the third closest luminaire.

Figure 12 The view from the observer point in Case 1, Otaranta, Espoo. The horizontal distances from the observer point to the five luminaires were 23.7, 60.0, 92.2, 125.1 and 158.3 m. The closest luminaire is not visible in this image.

Figure 13 The traffic condition for Cases 2 and 3 and view from the observer point in Case 2, Topeliuksenkatu, Helsinki. The horizontal distances from the observer point to the luminaires suspending on the same lane were 4.6, 31.4, 60.0, 89.0, 118.7, 147.6, 175.8 and 203.5 m. In Case 3, the distances were 2.4, 31.3, 60.0, 90.0, 118.6, 145.4 and 166.9 m. The two closest luminaire pairs are not visible in this image.

4.2.2 The experimental setup in observer longitudinal location and adaptation luminance study

In the second road lighting study (Publication IV), a series of luminance measurements were taken using an LMK Mobile Advanced imaging luminance photometer with a 55 mm focal length lens. The measurements were taken in Munkkiniemenranta, a street in Helsinki, Finland. Munkkiniemenranta (Figure 14. Munkkiniemenranta, Helsinki, Finland.) was lit by AEC Illuminazione LED-in 1H-ST 4.5-63 LED luminaires (103 W, 4000 K). The luminaires were pole-mounted on the right-hand side from the observer's point of view.

The S/P-ratio for the luminaire was 1.44. The distance between two adjacent poles was 30 metres, and the mounting height of the luminaires was 8.1 metres.

Luminance measurements were taken from inside a car in the driver's position. The observer's horizontal location on the ongoing lane was 2 metres from the right-hand side, as this could be considered as the driver's position. The imaging luminance photometer was at the height of 1.3 metres. Luminance measurements were taken from five measurement points (A, B, C, D, and E). The distance between two measurement points was 7.5 metres. The care used for measuring was stationed on the ongoing lane during the measurements. Depending on the measurement point, three or four street luminaires were present in the visual scene. Figure 14 and Figure 15 illustrate the measurement situation. During the measurement, there was a car stationed also on the oncoming lane but it had only the parking lights switched on. The LED-luminaires were dimmable using current reduction. The luminance measurements were repeated using three luminous flux levels: 100%, 70%, and 50%. The 70% and 50% luminous flux levels were obtained by current reduction.

Figure 14. Munkkiniemenranta, Helsinki, Finland.

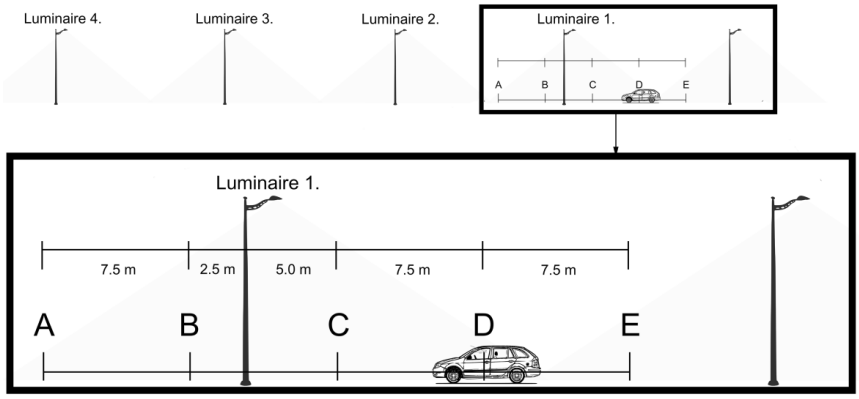

Figure 15 The measurement points A, B, C, D, and E and their positions and distances to the luminaires.

4.2.3 The measurement setup in experimenting methods for combining 3D laser scanning and luminance mapping

The location in the third road lighting experiment (Publication V) was Otaranta in Espoo, Finland. The location was the same as in Publications I, II, and III, but at the time of this experiment, Otaranta was lit using 100 W high-pressure sodium luminaires.

The laser scanner used was Faro Focus 3D, a terrestrial (TLS), 905 nm, phase-based, 305° × 360° field of view, continuous-wave laser scanner. At a distance of 25 m, the distance measurement accuracy for the laser scanner was ± 2 mm. The total size of the measured point cloud was 73 million points. The imaging luminance photometry was done using Nikon D800E digital camera, with 5.6 as the aperture value, ISO value of 100, and 8 s exposure time. The camera was luminance calibrated using an Optronic Laboratories Inc. model 455-6-1 reference luminance source.

4.3 Results

4.3.1 The results in adaptation field, veiling luminance, and adaptation luminance study

Twelve different adaptation fields were evaluated in the first road lighting study (Publication III). Two centre points were used in calculating the visual adaptation fields. The first centre point (centre 1) was the point in the middle of the lane at the end of the lane. This was the point to which a driver looks at with the largest probability [46, 47]. The second centre point (centre 2) was the horizontal centre point of the observer's lane surface exactly in the middle of two adjacent luminaires starting from 60 metres from the observer. The analysed adaptation fields included the 'road surface of the ongoing lane be-

tween two adjacent luminaires', 1°, 2°, 5°, 10°, 20°, 45°, and 90° circular adaptation fields, and 10°/20° elliptical adaptation field. For comparison, drivers' eye fixations over time tend to accumulate within a 10° circular field (centre 1) on a main road, and within a 10°/20° elliptical field (centre 1) on a residential street [47]. Figure 16, Figure 17, and Figure 18 illustrate the analysed visual adaptation fields in a luminance image in Topeliuksenkatu (Case 2).

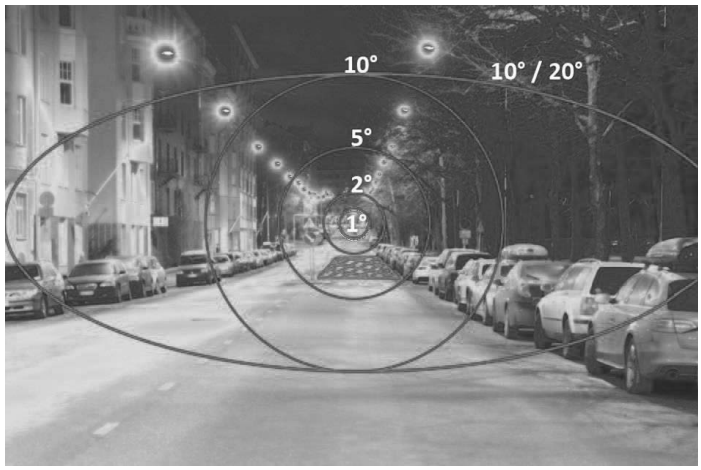

Figure 16. Luminance image of Case 2 illustrating the road surface adaptation field (centre 2), the circular adaptation fields of 1°, 2°, 5°, and 10° and the 10°/20° elliptical field centred at the end of the lane (centre 1). The image was taken with an LMK Mobile Advanced using a 55 mm focal length.

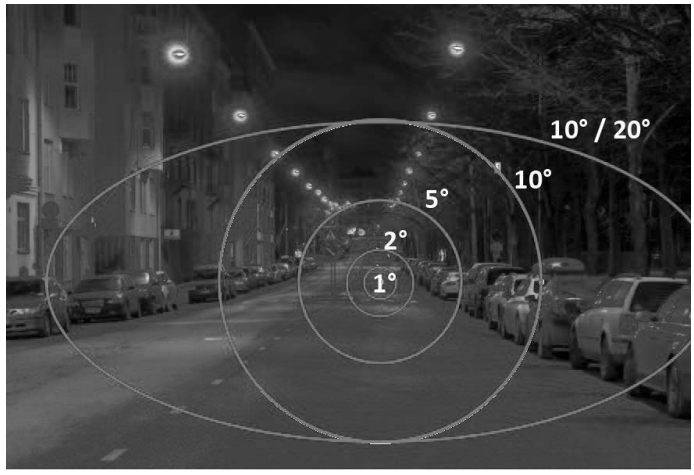

Figure 17. Luminance image of Case 2 illustrating the circular adaptation fields of 1°, 2°, 5°, and 10° and the 10°/20° elliptical field centred at the street's surface between two luminaires 60 metres from the observer (centre 2). The image was taken with an LMK Mobile Advanced using a 55 mm focal length.

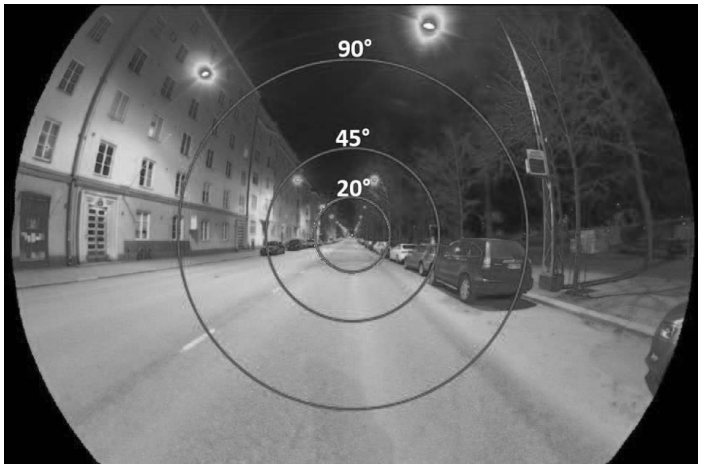

Figure 18. Luminance image of Case 2 illustrating the circular adaptation fields of 20°, 45°, and 90° centred at the end of the lane (centre 1). The image was taken with an LMK Mobile Advanced using an 8 mm focal length.

Table 1 presents the average mesopic luminances of the adaptation fields, excluding the circular fields of 45° and 90°. The mesopic values were converted from the measured photopic values using the CIE 191:2010 system for mesopic photometry.

Table 1 Average mesopic luminances (cdm^{-2}) for each adaptation field excluding the circular fields of 45° and 90°. The adaptation fields are described in the left-most column. $L_{ave,\ road}$ stands for the adaptation field on the road surface. The angle value stands for the size of the circular angle or the sizes of the elliptical angles. Centre 1 is the higher centre point in the lane's end, and centre 2 is the lower centre point on the road surface.

	Case 1	Case 2	Case 3
$L_{ave,\ road}$, centre 2	0.91	2.57	4.09
1° , centre 1	0.46	2.96	4.00
2° , centre 1	0.45	2.41	3.45
5° , centre 1	0.44	3.93	2.92
10° , centre 1	0.50	4.16	3.97
20° , centre 1	0.54	2.66	4.13
10°/20° , centre 1	0.41	4.57	3.01
10°/20° , centre 2	0.51	2.91	2.54
10° , centre 2	0.57	3.37	3.14
5° , centre 2	0.58	2.57	2.93
median	0.51	2.93	3.29
average mesopic	0.54	3.21	3.42
average photopic	0.50	3.24	3.45
σ	0.14	0.72	0.56
relative σ (%)	25.2%	22.5%	16.3%

The average relative standard deviation among the average mesopic luminances of the analysed adaptation fields was 21.3%. This could be considered a rather small deviation considering how different the compared adaptation fields were in terms of size, shape, and centre point. In Case 1, the luminance value of the road surface was much higher than in any other adaptation fields, being 78% higher than the median among the adaptation fields. In Cases 2 and 3, the difference between the 'road surface' adaptation field, and the circular and elliptical adaptation fields was not evident.

Large circular adaptation fields of 45° and 90° were analysed, and found problematic. When using adaptation fields of 45° and 90°, the high-luminance light sources often caused a lens flare in the imaging luminance measurements. The lens flare would then cause unavoidable measurement bias, and make the results unreliable.

Case 3 offered a chance to measure the luminance difference between a street bordered by buildings and a street bordered by a park. Table 2 presents the average luminances of the vertically halved adaptation fields of 10°, and 10°/ 20° in Case 3 (see Figure 19). The average luminances of the right side represent a street bordered by buildings and the average luminances of the left side represent a street bordered by a park. The average luminances of the building side were 48%, and 45% higher in the 10°, and 10°/ 20° adaptation fields respectively compared to the park side. The average luminance of the road surface was 76% and 113% higher than the average luminances of the park side adaptation fields. Furthermore, the average luminance of the road surface was 19% and 47% higher than the average luminances of the building side adaptation fields. If only the road surface is used as the adaptation field, the differences the bordering areas cause to adaptation luminance are neglected.

Table 2. Average photopic luminances (cdm^{-2}) for adaptation fields of 45°, and 90°. $MIAF_{45}$ stands for median in adaptation fields < 45°.

	Case 1	Case 2	Case 3
45°	2.56	4.68	4.74
90°	0.89	2.93	2.82
$MIAF_{45}$	0.48	2.97	3.32
$MIAF_{45}$ + L_{veil} (equation 4)	0.61	4.33	4.30

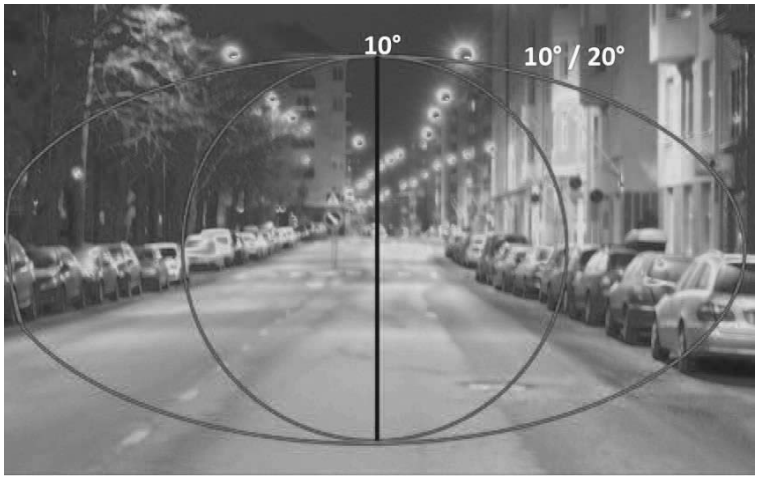

Figure 19. Adaptation fields of 10°, and 10°/ 20° in Case 3 halved to the building side and the park side.

Three adaptation fields in this analysis had their centre point both at the lane end (centre 1) and at the street surface in the middle of two adjacent luminaires (centre 2). These adaptation fields were 5° and 10° circular, and 10°/20° elliptical fields. The centre point on the street surface was only 1.1° lower from the observer's point of view than the centre at the lane end. Still, the average luminances of these comparable luminance fields differed noticeably depending on the centre point. In Case 1, the adaptation fields with the lower centre point (centre 2) had their average luminance value 18.7% higher on average than when the centre was at the lane end (centre 1). In Cases 2 and 3, the corresponding ratios were -29.5% and -11.8% respectively. This may suggest, that in more open and rural areas, a centre point on the road surface increases the average luminance of the adaptation field, and a centre at the lane end decreases it. In urban areas with buildings bordering the street, this would be vice versa. This observation may also be due to the luminaire used. In Case 1, the luminaire used was an LED luminaire, which has its light distribution more directed only to the road surface than the HPS luminaire in Cases 2 and 3.

In this first road lighting study, the term 'adaptation state' meant the luminance that the retina is adapted to. It was considered as the sum of the measured photopic average luminance of the adaptation field, L_p, and the veiling luminance, L_{veil}. In addition, the adaptation field and the area of measurement were considered to be the same area in the visual scene. The increment to the adaptation state caused by the veiling luminance depended on the fixation point and the veiling luminance model used. However, the differences of different veiling luminance model, fixation point, and adaptation field combinations were subtle. The adaptation states are presented in Tables 3, 4 and 5.

The average increments to adaptation luminance caused by adding veiling luminance were 29%, 35% and 24% in Cases 1, 2 and 3, respectively.

Table 3. The average luminance (in cdm^{-2}) of the adaptation field, L_p, and the adaptation state, $L_p + L_{veil}$, as the sum of the average luminance of the adaptation field and the veiling luminance for Case 1. The increment to the adaptation state caused by the veiling luminance depends on the veiling luminance model used. The average increment among the models is presented on the lower-most row for each adaptation field. $L_{ave,\ road}$ stands for the adaptation field on the road surface. The angle value stands for the size of the circular angle or the sizes of the elliptical angles. Centre 1 stands for the centre point at the end of the lane, and centre 2 stands for the lower centre point at the road surface.

Case 1	$L_{ave,\ road}$, centre 2	1° , centre 1	2° , centre 1	5° , centre 1	10° , centre 1	20° , centre 1	10°/20° , centre 1	10°/20° , centre 2	10° , centre 2	5° , centre 1
L_p	0.87	0.43	0.42	0.41	0.47	0.50	0.38	0.48	0.53	0.54
$L_p + L_{veil}$ using equation (9)	0.97	0.56	0.55	0.54	0.60	0.63	0.51	0.58	0.63	0.64
$L_p + L_{veil}$ using equation (4) , A=43, p = 0.9	0.99	0.55	0.54	0.53	0.59	0.62	0.50	0.57	0.62	0.63
$L_p + L_{veil}$ using equation (5)	1.08	0.64	0.63	0.62	0.68	0.71	0.59	0.63	0.68	0.69
average increase by L_{veil} to adaptation state	16.4%	35.4%	36.3%	37.2%	32.4%	30.5%	40.1%	23.5%	21.3%	20.9%

Table 4. The average luminance (in cdm^{-2}) of the adaptation field, L_p, and the adaptation state, $L_p + L_{veil}$, as the sum of the average luminance of the adaptation field and the veiling luminance for Case 2. The increment to the adaptation state caused by the veiling luminance depends on the veiling luminance model used. The average increment among the models is presented on the lower-most row for each adaptation field. $L_{ave,\ road}$ stands for the adaptation field on the road surface. The angle value stands for the size of the circular angle or the sizes of the elliptical angles. Centre 1 stands for the centre point at the end of the lane, and centre 2 stands for the lower centre point at the road surface.

Case 2	$L_{ave,\ road}$, centre 2	1° , centre 1	2° , centre 1	5° , centre 1	10° , centre 1	20° , centre 1	10°/20° , centre 1	10°/20° , centre 2	10° , centre 2	5° , centre 1
L_p	2.60	2.99	2.45	3.95	4.17	2.70	4.58	2.95	3.40	2.60
$L_p + L_{veil}$ using equation (9)	3.54	4.35	3.81	5.31	5.53	4.06	5.94	3.88	4.33	3.54
$L_p + L_{veil}$ using equation (4) , A=43, p = 0.9	3.27	3.93	3.40	4.89	5.12	3.64	5.52	3.61	4.06	3.27
$L_p + L_{veil}$ using equation (5)	3.59	4.42	3.89	5.38	5.61	4.13	6.01	3.94	4.39	3.59
average increase by L_{veil} to adaptation state	33.2%	41.7%	50.9%	31.6%	29.9%	46.2%	27.2%	29.3%	25.4%	33.2%

Table 5. The average luminance (in cdm^{-2}) of the adaptation field, L_p, and the adaptation state, $L_p + L_{veil}$ as the sum of the average luminance of the adaptation field and the veiling luminance for Case 3. The increment to the adaptation state caused by the veiling luminance depends on the veiling luminance model used. The average increment among the models is presented on the lower-most row for each adaptation field. $L_{ave,\ road}$ stands for the adaptation field on the road surface. The angle value stands for the size of the circular angle or the sizes

of the elliptical angles. Centre 1 stands for the centre point at the end of the lane, and centre 2 stands for the lower centre point at the road surface.

Case 3	$L_{ave,\ road}$, centre 2	1° , centre 1	2° , centre 1	5° , centre 1	10° , centre 1	20° , centre 1	10°/20° , centre 1	10°/20° , centre 2	10° , centre 2	5° , centre 1
L_p	4.11	4.02	3.47	2.96	3.99	4.15	3.04	2.58	3.17	2.97
$L_p + L_{veil}$ using equation (9)	4.79	5.00	4.45	3.93	4.97	5.13	4.02	3.26	3.85	3.65
$L_p + L_{veil}$ using equation (4) , A=43, p = 0.9	4.59	4.71	4.16	3.64	4.68	4.84	3.73	3.07	3.66	3.46
$L_p + L_{veil}$ using equation (5)	4.86	5.11	4.56	4.05	5.08	5.24	4.13	3.33	3.93	3.72
average increase by L_{veil} to adaptation state	15.6%	22.9%	26.5%	31.1%	23.0%	22.1%	30.2%	24.9%	20.2%	21.0 %

The mesopic luminance, L_{mes}, of the area of measurement can be calculated using the CIE 191:2010 system for mesopic photometry when we know the measured photopic luminance, L_p, and the S/P ratio of the luminaire [2]. The veiling luminance is an increment to the adaptation state, but it does not increase the average luminance of the area of measurement. The true mesopic luminance value, $L_{mes,true}$, was the mesopic luminance value that was calculated taking the veiling luminance into account. Furthermore, $L_{mes,true}$ was interpolated from between the originally calculated mesopic luminance value, L_{mes}, and the measured photopic luminance value, L_p. In this study, the interpolation was done using the iterative process of mesopic luminance calculation as described in the CIE 191:2010 system for mesopic photometry (Equations 1 and 2) [2]. Both mesopic values for the area of measurement, L_{mes} and $L_{mes,true}$, were calculated. Then, the increment or the decrement of the veiling luminance caused to the $L_{mes,true}$ compared to L_{mes} was calculated. The average differences caused by veiling luminance were -0.6%, 0.6% and 0.5% in Cases 1, 2 and 3, respectively. It was notable that even though the veiling luminances increased the adaptation states by 29%, 35% and 24% in Cases 1, 2 and 3, respectively, the effect on the calculated mesopic luminances in the area of measurement was much smaller. If the S/P ratio of the luminaires is more than one, the veiling luminance will decrease the true mesopic luminances, and if the S/P ratio of the luminaires is less than one, the veiling luminance will increase the true mesopic luminances. In this study, the largest decrement was -1.3% found in Case 1, and the highest increment was 1.0% found in Case 2. All of the mesopic luminance combinations (in Cases 1, 2 and 3; with Equations 7, 2 and 3; and every adaptation field), and the differences between L_{mes} and $L_{mes,true}$ are presented in Tables 6, 7, and 8.

Table 6. The mesopic luminances, L_{mes} (in cdm^{-2}), and the mesopic luminances influenced by veiling luminance, $L_{mes,true}$, calculated with the three veiling luminance models for each adaptation field in Case 1. Differences 1, 2 and 3 present the difference (in percentage) between the original mesopic luminance and the mesopic luminances influenced by veiling luminance using the veiling luminance models 9, 4 and 5 respectively. $L_{ave,\ road}$ stands for the adaptation field on the road surface. The angle value stands for the size of the circular angle or the sizes of the elliptical angles. Centre 1 is the higher centre point at the lane's end, and centre 2 is the lower centre point on the road surface.

Case 1	L_{mes}	$L_{mes,true}$ equation (9)	$L_{mes,true}$ equation (4)	$L_{mes,true}$ equation (5)	differ-ence 1	differ-ence 2	differ-ence 3
$L_{ave,\ road}$, centre 2	0.9144	0.9129	0.9125	0.9112	-0.2%	-0.2%	-0.4%
1° , centre 1	0.4630	0.4602	0.4606	0.4575	-0.6%	-0.5%	-1.2%
2° , centre 1	0.4526	0.4498	0.4493	0.4471	-0.6%	-0.7%	-1.2%
5° , centre 1	0.4422	0.4394	0.4389	0.4368	-0.6%	-0.8%	-1.2%
10° , centre 1	0.5044	0.5017	0.5012	0.4990	-0.5%	-1.1%	-1.1%
20° , centre 1	0.5355	0.5328	0.5323	0.5301	-0.5%	-0.6%	-1.0%
10°/20° , centre 1	0.4110	0.4081	0.4077	0.4055	-0.7%	-0.8%	-1.3%
10°/20° , centre 2	0.5148	0.5129	0.5125	0.5111	-0.4%	-0.5%	-0.7%
10° , centre 2	0.5664	0.5646	0.5642	0.5628	-0.3%	-0.4%	-0.6%
5° , centre 2	0.5767	0.5749	0.5745	0.5731	-0.3%	-0.4%	-0.6%

Table 7. The mesopic luminances, L_{mes} (in cdm^{-2}), and the mesopic luminances influenced by veiling luminance, $L_{mes,true}$, calculated with the three veiling luminance models for each adaptation field in Case 2. Differences 1, 2 and 3 present the difference (in percentage) between the original mesopic luminance and the mesopic luminances influenced by veiling luminance using the veiling luminance models 9, 4 and 5, respectively. $L_{ave,\ road}$ stands for the luminance of the adaptation field on the road surface. The angle value stands for the size of the circular angle or the sizes of the elliptical angles. Centre 1 is the higher centre point at the lane's end, and centre 2 is the lower centre point on the road surface.

Case 2	L_{mes}	$L_{mes,true}$ equation (9)	$L_{mes,true}$ equation (4)	$L_{mes,true}$ equation (5)	differ-ence 1	differ-ence 2	differ-ence 3
$L_{ave,\ road}$, centre 2	2.5650	2.5788	2.5832	2.5840	0.5%	0.7%	0.7%
1° , centre 1	2.9559	2.9740	2.9802	2.9812	0.6%	0.8%	0.8%
2° , centre 1	2.4133	2.4316	2.4375	2.4385	0.8%	1.0%	1.0%
5° , centre 1	3.9260	3.9435	3.9453	3.9453	0.4%	0.5%	0.5%
10° , centre 1	4.1555	4.1710	4.1710	4.1710	0.4%	0.4%	0.4%
20° , centre 1	2.6627	2.6809	2.6869	2.6879	0.7%	0.9%	0.9%
10°/20° , centre 1	4.5713	4.5795	4.5795	4.5795	0.2%	0.2%	0.2%
10°/20° , centre 2	2.9125	2.9260	2.9304	2.9313	0.5%	0.6%	0.6%
10° , centre 2	3.3695	3.3828	3.3873	3.3881	0.4%	0.5%	0.5%
5° , centre 2	2.5650	2.5788	2.5832	2.5840	0.5%	0.7%	0.7%

Table 8. The mesopic luminances, L_{mes} (in cdm^{-2}), and the mesopic luminances influenced by veiling luminance, $L_{mes,true}$, calculated with the three veiling luminance models for each adaptation field in Case 3. Differences 1, 2 and 3 present the difference (in percentage) between the original mesopic luminance and the mesopic luminances influenced by veiling luminance using the veiling luminance models 9, 4 and 5, respectively. $L_{ave,\ road}$ stands for the adaptation field on the road surface. The angle value stands for the size of the circular angle or the sizes of the elliptical angles. Centre 1 is the higher centre point at the lane's end, and centre 2 is the lower centre point on the road surface.

Case 3	L_{mes}	$L_{mes,true}$ equation (9)	$L_{mes,true}$ equation (4)	$L_{mes,true}$ equation (5)	differ-ence 1	differ-ence 2	differ-ence 3
$L_{ave,\ road}$, centre 2	4.0899	4.0996	4.1030	4.1042	0.2%	0.3%	0.3%
1° , centre 1	4.0025	4.0157	4.0205	4.0205	0.3%	0.4%	0.4%

2° , centre 1	3.4458	3.4594	3.4642	3.4659	0.4%	0.5%	0.6%
5° , centre 1	2.9233	2.9372	2.9419	2.9437	0.5%	0.6%	0.7%
10° , centre 1	3.9697	3.9830	3.9877	3.9883	0.3%	0.5%	0.5%
20° , centre 1	4.1336	4.1468	4.1495	4.1495	0.3%	0.4%	0.4%
10°/20° , centre 1	3.0103	3.0242	3.0289	3.0306	0.5%	0.6%	0.7%
10°/20° , centre 2	2.5434	2.5540	2.5574	2.5586	0.4%	0.5%	0.6%
10° , centre 2	3.1409	3.1511	3.1546	3.1558	0.3%	0.4%	0.5%
5° , centre 2	2.9342	2.9446	2.9480	2.9492	0.4%	0.5%	0.5%

4.3.2 The results in observer longitudinal location and adaptation luminance study

In the second road lighting study (Publication IV), the relation between the observer's longitudinal location and the adaptation luminance was examined. Firstly, the average luminances of circular adaptation fields of 1°, 2°, 5°, 10° and the 'road surface' were measured at measurement points A, B, C, D and E (Figure 20 and Figure 21). Then, the veiling luminances were calculated for 25 different longitudinal locations (Figure 22).The adaptation state calculations were only executed applying a 5° circular adaptation field, as the differences among the different adaptation fields were small in terms of the longitudinal variation. Furthermore, most of the analysis was done with the 100% lamp luminous flux level data (no current reduction), as the results from different dimming levels were relatively similar, i.e., excluding the obvious scaling difference.

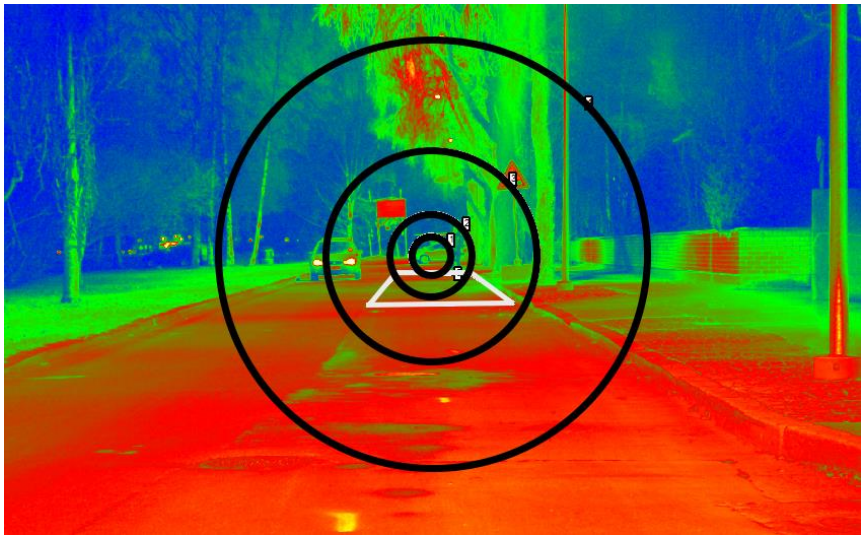

Figure 20 A luminance image of Munkkiniemenranta showing the circular adaptation fields of 1°, 2°, 5°, 10° and the street surface between two adjacent luminaire poles. This luminance image was taken at measurement point **D**.

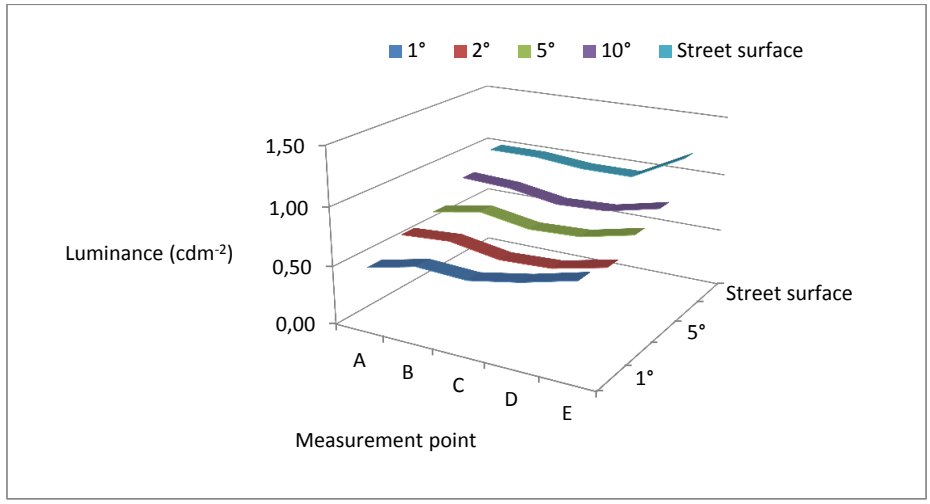

Figure 21 The average luminances of circular visual adaptation fields of 1°, 2°, 5°, 10° and the road surface in measurement points A, B, C, D and E. Luminaires were at 100% intensity.

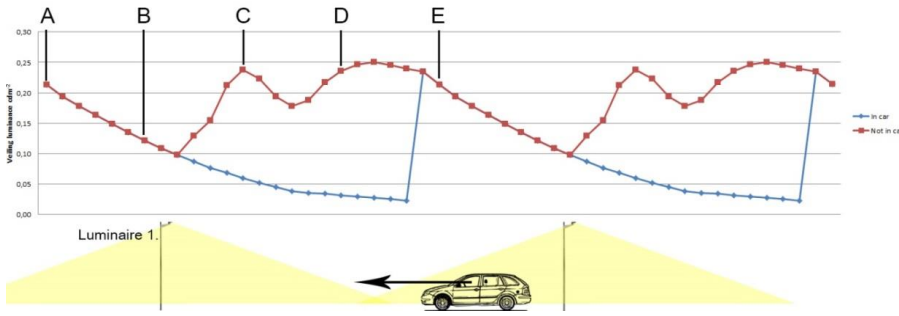

Figure 22 The repeating pattern of veiling luminance calculation points and the calculated veiling luminance for each point. The red plot (not in car) illustrated the veiling luminance values of the unblocked visual field. The blue plot (In car) illustrates the veiling luminances when the screening plane is 20° to the horizontal.

The differences of the average luminances among different adaptation fields were moderate. The average relative standard deviation among the average luminances of the adaptation fields was 22%. The differences in the circular adaptation field were very small. The road surface had systematically slightly higher average luminance values than the circular adaptation fields. In addition, the larger circular adaptation fields had higher average luminances than the smaller circular fields. The longitudinal location had a small effect on the average luminance of the adaptation field. The average relative standard deviation among the measurement points was 9%.

Veiling luminance was strongly dependent on location. In the most extreme case, the veiling luminance increased over 900% within 1.25 m difference in longitudinal position. This occurred when the observer was considered to be inside a car, and the light sources, which are at higher angles than 20° from the observer's horizontal fixation, were not included. When the field of view

was unblocked, the variance was not as dramatic as in the 'in car' case. Nevertheless, when the field of view was non-screened, the maximum to minimum ratio of veiling luminances was 2.61.

Adaptation luminance was considered as the sum of the average luminance of the adaptation field and the veiling luminance. Furthermore, adaptation luminance determined the spectral responsiveness of the retina. In Publication III and IV, the area of measurement (AOM) and the adaptation field were considered the same area within the visual field. Figure 23 shows the increment to the adaptation luminance caused by the veiling luminance when not in the car. The average luminance values for the adaptation fields between the measurement points A, B, C, D and E were linearly interpolated. On the average, veiling luminance increased the adaptation luminance by 25%.

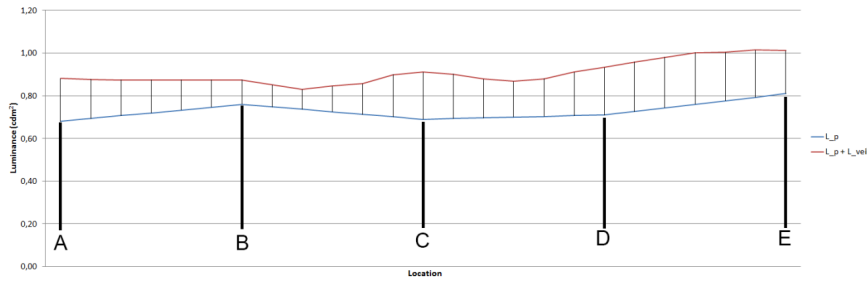

Figure 23 The increment to the adaptation luminance caused by the veiling luminance. Blue line represents the average luminance of the adaptation field, and the red line represents the adaptation luminance. A, B, C, D and E are the measurement points.

As in the previous subchapter (4.3.1), the mesopic values, L_{mes}, and the true mesopic values, $L_{mes,true}$, were calculated for the areas of measurement. The average proportional bias caused by veiling luminances was -0.56%. This can be considered very small. Finally, the set of $L_{mes,true}$ values in different longitudinal locations was analysed. The relative standard deviation among the $L_{mes,true}$ values was 4.4%.

4.3.3 Results in experimental methods for combining 3D laser scanning and luminance mapping

In Publication V, the luminance 3D point clouds were created by integrating the terrestrial laser scan data sources with the luminance values derived from digital images. The generated 3D data enabled the evaluation of the luminances according to their location or position on the road. Figure 24 presents the measured luminance values, the measurement points (P1-P4), and the locations of the street luminaires (L1-L5).

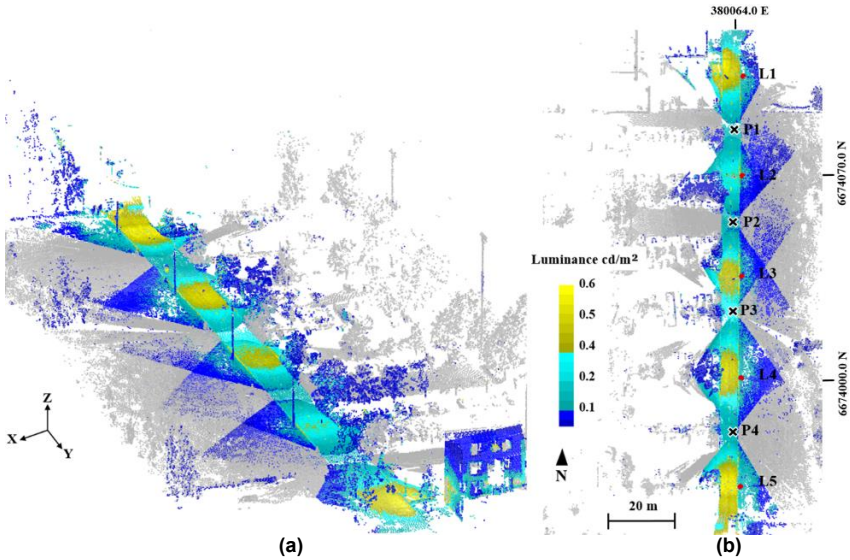

Figure 24. The measured 3D luminance data of Otaranta; **(a)** bird's-eye view and **(b)** 2D orthographic view, from above. The positions of the scan and image stations are marked with black crosses (P1–P4) and street luminaires are marked with red dots (L1–L5). (From Publication V)

The luminance values were measured towards two directions, northbound and southbound, and sampled by calculating an average value for 10 × 10c m areas. From the luminance value point cloud, values were derived for average luminance, $L_{road,ave}$, overall uniformity, U_o, and longitudinal uniformity, U_i, for three road sections next to luminaires 2, 3 and 4. The overall uniformity, U_o, and longitudinal uniformity, U_i, acquirement followed approximately the EN-13201 standard [45]. The $L_{road,ave}$ and U_i values were calculated for a 20 × 0.1 m longitudinal area in the middle of a lane. U_o was calculated for 20 × 2.0 m area of a single lane. The standard deviation for the measured luminances on the right lane was 0.029 cd/m², and for the left lane 0.036 cd/m². Table 9 presents the measured values for measurement points P1 - P4.

Table 9. The comparison of the road surface luminance measured facing northbound and southbound directions (N and S). Average luminance ($L_{road,ave}$), Overall Uniformity of luminance (U_o) and Longitudinal Uniformity (U_i) values were derived for three road sections next to street luminaires L2, L3 and L4. $L_{road,ave}$ and U were calculated separately for the left and right lane.

Direction (/Position)	$L_{road,ave}$, left lane (cd/m²)	$L_{road,ave}$, right lane (cd/m²)	U_o (%)	U_i, left lane (%)	U_i, right lane (%)
S (P1)	0.211	0.221	0.425	0.286	0.267
N (P2)	0.206	0.214	0.433	0.385	0.286
S (P2)	0.316	0.307	0.446	0.368	0.389
N (P3)	0.298	0.280	0.396	0.389	0.353
S (P3)	0.383	0.369	0.495	0.478	0.500
N (P4)	0.346	0.346	0.399	0.318	0.364

4.4 Summary

The differences among adaptation luminances, when the adaptation field varied in terms of size, shape and centre point, were quantified. The average standard deviation among all of the average luminances of the adaptation fields was 21%. Veiling luminances increased the adaptation luminance by 29% on the average. Veiling luminances increase the adaptation luminance but not the luminance in the measurement area. This induces a difference in mesopic luminance calculation, depending on whether the veiling luminances are taken into account or not. The difference between the mesopic luminances, calculated with and without the influence of veiling luminances, was |0.6% |on average.

We quantified the effect that the observer's longitudinal location has on the adaptation luminance and the mesopic luminance in the area of measurement. On average, among the longitudinal locations, veiling luminance increased the adaptation luminance by 25%. The location-dependent relative standard deviation among the calculated mesopic luminance values was 4.4%.

Combining luminance measurements to terrestrial laser scanning point clouds gave promising results. The method for the data integration was found successful. When a luminance value is connected to a 3D location, the distance and the angle between the observer and the luminance source can be easily measured for numerous observer positions. This enables more accurate and versatile road lighting measurement.

5. Conclusions and discussion

The adaptation luminance cannot yet be accurately determined, when the luminance distribution of the visual environment is non-uniform. Without knowing the *accurate* adaptation luminance, the CIE 191 system for mesopic photometry cannot be applied to achieve an *accurate* mesopic luminance value. Fortunately, the practical road lighting measurements and design may be more forgiving, and may not necessarily demand an absolutely accurate adaptation luminance. For example, the effect of veiling luminance on the final mesopic luminance value was found to be small enough to be covered by a small ±2% tolerance in the road lighting regulations.

This thesis included studies of two kind: contrast threshold experiments in *simulated* road lighting conditions (I & II) and adaptation luminance analyses in *real* road lighting conditions (III – V). In the contrast threshold experiments, circular targets (1.5°) were gradually presented to the test subjects, and the contrast threshold at the moment of the target detection was measured. The contrast threshold was compared to a 3° circular field behind and encompassing the target. The term 'complexity' was coined to represent the relative difference between the minimum luminance and the average luminance of the target's encompassing background (5°), or in other words, how uniform or non-uniform the encompassing background was. The experiments showed that the 'complexity' of the target's background hindered the visual performance, as it increased the contrast threshold. When the target's background was virtually uniform, contrast threshold was significantly lower than when the encompassing background was complex. In addition, the results supported the local adaptation hypothesis, in which different retinal coordinates are considered to adapt independently. However, it remained impossible to clearly distinguish which part of the visual performance was physiological adaptation and which part was cognitive processing. Thus, the contrast threshold experiments did not provide sound evidence that would directly help to define how to determine the adaptation luminance.

The first objective of this thesis was to quantify the increment or the decrement in the adaptation luminance, caused by luminance differences in the visual field. The adaptation luminance could not be completely quantified by the contrast threshold experiments, as the discrimination between the physiological adaptation and the cognitive part of visual performance was not possible. However, the results showed that the luminance distribution non-uniformities

increase the contrast threshold, and that different retinal coordinates adapt locally and independently.

In publications III and IV, the average luminances were measured for visual adaptation fields that varied in terms of size, shape and location. The measured values were summed with the corresponding veiling luminance to determine the adaptation luminance. Excluding the effect of veiling luminance, the determined adaptation luminance did depend on the size, shape, or location of the adaptation field, but rather moderately. Thus, no knowledge was gained by comparing the different adaptation fields that would aid to directly define the determination of adaptation luminance. In publication III, the relative standard deviation among the compared average luminances of the adaptation fields was 21%. The veiling luminance increased the adaptation luminance by 29% and 25% in publications III and IV respectively. The luminance values of the areas of measurement were converted from photopic to mesopic applying the determined adaptation luminances. In this conversion, the difference in mesopic luminance caused by taking the veiling luminance into account was found very small, only |0.6%| in publication III. In publication IV, the average difference in the photopic and the mesopic luminance value was only 4.4%, even when the effect of longitudinal location and the veiling luminance was combined. In CIE work group JTC-1, the effect of veiling luminance on the adaptation luminance is being defined. For this definition, the JTC-1 can utilise the calculations from the real road lighting environment found in Publications III and IV.

Publication V confirmed as plausible a novel measurement method, where 3D laser scanning and imaging luminance photometry are combined. In the method, a data point-cloud included the distances and the directions between the observer and the road surface, or the observer and a high-luminance source. Hence, the method enables the analysis of the veiling luminance at the observer location, and the reflection behaviour of the road surface.

Several further studies are needed before the adaptation luminance can be accurately determined. Firstly, no veiling luminance model can yet be utilised for an arbitrary retinal location. Secondly, the effect of constantly changing visual environment should be quantified, as the traffic is constant movement. Thirdly, the physiological adaptation and the cognitive processing should be separated in terms of visual performance. This may be difficult via human subject research, but modelling and simulating a human eye could be a more auspicious approach.

The experiments in this thesis showed, that even though the veiling luminance increased the adaptation luminance by a noticeable amount (29%), this caused only a minuscule difference (|0.6%|) to the final mesopic luminance. Thus, a small ±2% tolerance in the road lighting regulations would cover most of the variation in mesopic luminance caused by the veiling luminance. Furthermore,

the findings in this study indicate that adaptation occurs independently in different retinal coordinates, rather than the retina being adapted to a single adaptation luminance as an entity. If adaptation is thoroughly a local phenomenon on the retina, the luminance value in each coordinate of the visual field can be used as an initial value for the adaptation luminance of a corresponding retinal coordinate. This initial value for adaptation luminance can be further defined by also considering the effect of veiling luminance, eye movement and the movement of the traffic environment. Furthermore, if adaptation is local, the average luminance of the area of measurement can be used as an approximation for the adaptation luminance. Thus, also in CIE work group JTC-1, the emphasis can be shifted towards defining how the veiling luminance, the eye movements and the traffic movement alter the adaptation luminance for the retinal coordinates equivalent to the area of measurement.

For an *accurate* determination of adaptation luminance, at least the effect of veiling luminance and the effect of luminously non-uniform and mutable visual environment should be considered and further analysed. In practical road lighting design and measurements, the luminance in the area of measurement is a passable estimation for the adaptation luminance.

References

[1] M. Puolakka and L. Halonen, "CIE and mesopic photometry," in *Proceedings of 27th Session of the CIE*, Sun City, pp. 3-9, South Africa, 2011.

[2] "Recommended system for mesopic photometry based on visual performance," CIE 191:2010, Vienna, 2010.

[3] T. Young, "The bakerian lecture: On the theory of light and colours," *Philosophical transactions of the royal society of London*, vol. 92, pp. 12-48, January 1802.

[4] G. Østerberg, "Topography of the layer of rods and cones in the human retina," *Acta ophthalmologica*, vol. 6, 1935.

[5] H. Laurens, "Studies on the relative physiological value of spectral lights. IV. The visibility of radiant energy," *Americal journal of physiology*, vol. 67, pp. 348-365, 1924.

[6] "Photopic luminous efficiency function," *Principales décisions de la Commission Internationale de l'Eclairage*, 6th session, Geneve, July 1924.

[7] B. H. Crawford, "The scotopic visibility function," *Proceedings of the Physical Society*, vol. 62, no. 5, pp. 321-334, 1949.

[8] "Photometry - the CIE system of physical photometry," Commission Internationale de l'Eclairage Standard CIE S 010/E:2004, CIE, Vienna, 2004.

[9] J. A. Smith Kinney, "Comparison of scotopic, mesopic, and photopic spectral sensitivity curves," *Journal of the Optical Society of America*, vol. 48, no. 3, pp. 185-190, March 1958.

[10] D. A. Palmer, "A system of mesopic photometry," *Nature*, vol. 209, pp. 276-281, January 15th 1966.

[11] H. Shimozono and M. Ikeda, "Spectral luminous efficiency functions in the mesopic range," *Journal of the Optical Society of America A*, vol. 71, no. 3, pp. 280-284, March 1981.

[12] K. Takeichi and K. Sagawa, "Mesopic luminous-efficiency functions," *Journal of the Optical Society of America A*, vol. 3, no. 1, pp. 71-75, January 1986.

[13] I. Mitsuo and H. Yaguchi, "Subadditivity and superadditivity in heterochromatic brightness matching," *Vision Research*, vol. 23, no. 12, pp. 1711-1718, 1983.

[14] R. Clear and S. Berman, "Additivity constraints and visual task considerations in mesopic photometry," *Journal of the Illuminating Engineering Society*, pp. 90-104, 2001.

[15] J. Ketomäki, P. Orreveteläinen, L. Halonen, and M. Eloholma, "Visual performance in night-time driving," *Ophthalmic and Physiological Optics*, vol. 26, pp. 254-263, 2006.

[16] J. D. Bullough, J. P. Freyssinier-Nova, A. Bierman, and M. S. Rea, "A proposed unified system of photometry," *Lighting Research and Technology*, vol. 36, no. 2, pp. 85-111, May 2004.

[17] M. A. Webster, G. B. Stanley, A. A. Stocker, A. Kohn, T. O. Sharpee, O. Schwartz, and C. W. G. Clifford, "Visual adaptation: Neural, psychological and computational aspects," *Vision Research*, vol. 47, no. 25, pp. 3125-3131, November 2007.

[18] D. E. Spencer and P. Moon, "The specification of foveal adaptation," *Journal of Optical Society of America*, vol. 33, no. 8, pp. 444-456, 1943.

[19] "ILV: International lighting vocabulary," Standard CIE S 017/E:2011, Vienna, 2011.

[20] D. Jameson and L. Hurvich, "Spectral sensitivity of the fovea. I. Neutral adaptation," *Journal of the Optical Society of America*, vol. 43, no. 6, pp. 485-494, June 1953.

[21] L. Hurvich and D. Jameson, "Spectral sensitivity of the fovea. II. Dependence on chromatic adaptation," *Journal of Optical Society of America*, vol. 43, no. 7, pp. 552-559, July 1953.

[22] "Spectral effects of lighting on visual performance at mesopic lighting levels," Technical Memorandum TM-12-12, Illuminating Engineering Society of North America, New York, 2012.

[23] U. Stabell and B. Stabell, "Absolute spectral sensitivity at different eccentricities," *Journal of Optical Society of America*, vol. 71, no. 7, pp. 836-840, July 1981.

[24] E. E. Koldenhof, A. J. van Doorn, J. J. Koenderink, and J. A. van Esch, "Spectral sensitivity and wavelength discrimination of the human peripheral visual field," *Journal of Optical Society of America A*, vol. 1, no. 5, pp. 443-450, May 1984.

[25] W. J. de Haas, "On the diffraction phenomenon caused by a great number of irregularly distributed," *Proceedings of Huygens Institute - Royal Netherlands*

Academy of Arts and Sciences (KNAW), vol. 20, no. II, pp. 1278-1288, 1918.

[26] Y. Ohno and T. Uchida, "Effect of high luminance sources to peripheral adaptation state in mesopic range," in *Proceedings of CIE Centenary Conference "Towards a New Century of Light"*,pp. 529-539, Paris, 2013.

[27] L. L. Holladay, "The fundamentals of glare and visibility," *Journal of the Optical Society of America and review of scientific instruments*, vol. 12, no. 4, p. 1926, April 1926.

[28] B. H. Carwford and W.S. Stiles, "The effect of a glaring light source on extrafoveal vision," in *Proceedings of Royal Society Series B, Biological Sciences*, vol. 122, pp. 255–280, 1937.

[29] G. A. Fry, "A re-evaluation of the scatter theory of glare," *Journal of the Illuminating Engineering Society*, vol. 49, pp. 98-102, 1954.

[30] W. Adrian and A. Bhanji, "Fundamentals of disability glare: A formula to describe stray light in the eye as a function of glare angle and age," in *Proceedings of the First International Symposium on Glare*, pp. 185-193, New York, 1991.

[31] J. Vos, "On the cause of disability glare and its dependence on glare angle, age and ocular pigmentation," *Clinical and Experimental Optometry*, vol. 86, no. 6, pp. 363-370, November 2003.

[32] "CIE Equations for Disability Glare," CIE 146:2002, Vienna, 2002.

[33] Y. Ohno and T. Uchida, "Angular characteristics of the surrounding luminance effect on peripheral adaptation state in the mesopic range," in *Proceedings of CIE 2014 Lighting Quality and Energy Efficiency*, pp. 273 – 280, Kuala Lumpur, April 2014.

[34] H. S. Ginis, G. M. Perez, J. M. Bueno, A. Pennos, and P. Artal , "Wavelength dependence of the ocular straylight," *Visual Psychophysics and Physiological Optics*, vol. 54, no. DOI:10.1167/iovs.13-11697, pp. 3702–3708, April 2013.

[35] M. Ayama, R. Yamazaki, S. Nakanoya, T. Tashiro, T. Ishikawa, K. Ohnuma, H. Shinoda, and K. Araki, "Estimation of straylight in the eye and its relation to visual function," *Optical Review*, vol. 22, no. 2, pp. 185-196, April 2015.

[36] A. Hurden, P. Smith, G. Evans, A. Harlow, A. Bunting, and J. Barbur, "Visual performance at mesopic light levels: an empirical model," *Lighting Research and Technology,* vol. 31, no. 3, pp. 127-131, 1999.

[37] M. Leibenger and S. Raphael, "Models of mesopic photometry applied to the contrast threshold of peripheral and foveal objects," in *Proceedings of the 26th Session of the CIE*, pp. D1-38 - D1-41, Beijing, 2007.

[38] K. Narisada, "Visual perception in non-uniform fields," *Journal of Light and Visual Environment*, vol. 16, no. 2, pp. 81-88, 1992.

[39] I. J. Murray, W. N. Charman, and S. Plainis, "The role of retinal adaptation in night driving," *Optometry and vision science*, vol. 82, no. 8, pp. 682-688, 2005.

[40] K. Pearson, "Notes on regression and inheritance in the case of two parents," in *Proceedings of the Royal Society of London*, vol. 58, pp. 240-242, June 1895.

[41] F. Pestilli, G. Viera, and M. Carrasco, "How do attention and adaptation affect contrast sensitivity," *Journal of Vision*, vol. 30, no. 7, pp. 1-12, May 2007.

[42] R. Shapley and C. Enroth-Cugell, "Visual adaptation and retinal gain controls," in *Progress in Retinal Research,* vol. 3, ch. 9, pp. 263-346, 1984.

[43] Y. Lin, S. Fotios, M. Wei, and Y. Sun, "Eye movement and pupil size constriction under discomfort glare," *Investigative Ophthalmology & Visual Science*, vol. 56, no. 3, pp. 1649-1656, January 2015.

[44] W. S. Stiles, "Discussion on disability glare," in *CIE meeting in Scheveningen. Sekretariatsberichte der Zehnten Tagung*, Scheveningen, pp. 183-201, 1942.

[45] EN 13201-3, "Road lighting - part 3: Calculation of performance," European Committee for Standardization, Brussels, European Standard EN 13201-3, 2004.

[46] C. Cengiz, H. Kotkanen, M. Puolakka, O. Lappi, E. Lehtonen, L. Halonen, and H. Summala, "Combined eye-tracking and luminance measurements while driving on a rural road: Towards determining mesopic adaptation luminance," *Lighting Research and Technology*, 2013.

[47] J. Winter and S. Völker, "Typical eye fixation areas of car drivers in inner city environments," in *Proceedings of Lux Europa, 12th European Lighting Conference*, Krakow, 2013.

Appendices

Table 10.The target number, the corresponding horizontal and vertical eccentricities, photopic and mesopic average luminance of the target's background (3°), the mean contrast threshold among the subjects and the standard deviation of the contrast thresholds, the complexity value for the 5° circular field surrounding the target, and the percentage of missed targets. 'Low luminance' scene.

			'Low luminance' scene					
no	h (deg)	v (deg)	L_p (cd/m^2)	L_{mes} (cd/m^2)	CT	σ	comp.	miss (%)
1	-60	0	0.10	0.13	0.79	0.25	0.65	48
2	-45	0	0.12	0.16	0.71	0.26	0.30	26
3	-30	0	0.09	0.12	0.46	0.17	0.39	0
4	-20	0	0.28	0.34	0.72	0.26	0.58	33
5	-12	-16	1.56	1.67	0.19	0.08	0.47	0
6	-12	16	0.06	0.08	0.30	0.08	0.13	0
7	-10	0	0.26	0.32	0.52	0.18	0.71	0
8	-6	-8	1.60	1.70	0.17	0.05	0.83	0
9	-6	8	0.08	0.11	0.30	0.10	0.32	0
10	-2	-20	2.80	2.90	0.12	0.07	0.59	0
11	0	-10	2.80	2.90	0.08	0.03	0.70	0
12	0	0	0.14	0.18	0.43	0.16	0.75	3
13	1	10	0.09	0.12	0.22	0.08	0.86	0
14	0	20	0.08	0.11	0.60	0.29	0.92	25
15	6	-8	1.05	1.15	0.61	0.19	0.92	4
16	6	8	0.07	0.10	0.24	0.10	0.50	0
17	10	0	0.11	0.14	0.56	0.19	0.38	0
18	12	-16	2.75	2.85	0.33	0.19	0.76	17
19	12	16	0.07	0.10	0.24	0.16	0.25	0
20	20	0	0.08	0.11	0.21	0.07	0.25	0
21	30	0	0.07	0.1	0.29	0.10	0.10	0
22	45	0	0.09	0.12	0.28	0.11	0.10	0
23	60	0	0.10	0.13	1.01	0.00	0.16	96

Table 11. The target number, the corresponding horizontal and vertical eccentricities, photopic and mesopic average luminance of the target's background (3°), the mean contrast threshold among the subjects and the standard deviation of the contrast thresholds, the complexity

value for the 5° circular field surrounding the target, and the percentage of missed targets. 'High luminance' scene.

			High luminance image					
no	h (deg)	v (deg)	L_p (cd/m^2)	L_{mes} (cd/m^2)	CT	σ	comp.	miss (%)
1	-60	0	0.22	0.27	0.99	0.08	0.68	88
2	-45	0	0.27	0.33	0.77	0.28	0.31	46
3	-30	0	0.20	0.25	0.46	0.25	0.36	7.4
4	-20	0	0.66	0.75	0.72	0.27	0.60	33
5	-12	-16	3.83	3.89	0.22	0.13	0.44	0
6	-12	16	0.15	0.19	0.29	0.14	0.11	0
7	-10	0	0.61	0.70	0.68	0.22	0.70	13
8	-6	-8	4.24	4.28	0.20	0.15	0.81	0
9	-6	8	0.20	0.25	0.29	0.10	0.38	0
10	-2	-20	6.40	6.40	0.16	0.11	0.86	24
11	0	-10	7.00	7.00	0.07	0.03	0.76	0
12	0	0	0.39	0.46	0.32	0.09	0.73	0
13	1	10	0.21	0.26	0.31	0.15	0.87	0
14	0	20	0.17	0.21	0.54	0.29	0.95	24
15	6	-8	2.30	2.41	0.58	0.23	0.91	4
16	6	8	0.17	0.21	0.23	0.11	0.49	0
17	10	0	0.28	0.34	0.40	0.26	0.36	0
18	12	-16	5.75	5.75	0.27	0.13	0.77	43
19	12	16	0.16	0.20	0.23	0.18	0.21	0
20	20	0	0.21	0.26	0.21	0.07	0.22	0
21	30	0	0.16	0.20	0.25	0.10	0.08	0
22	45	0	0.20	0.25	0.27	0.20	0.26	4
23	60	0	0.23	0.28	1.00	0.03	0.15	96

Table 12. The target number and the corresponding horizontal and vertical eccentricities. The average luminance of the target's background (3°), the mean contrast threshold among the subjects and the standard deviation of the contrast thresholds, and the percentage of missed targets for both the original scene and the modified scene. 'Low luminance' scene.

	low luminance		Original scene				Modified scene			
no	h (deg)	v (deg)	L (cd/m2)	CT	σ	miss (%)	L (cd/m2)	CT	σ	miss (%)
1	-75	0	0,1	1,0	0,00	100	0,09	0,94	0,15	79,17
2	-60	0	0,1	0,79	0,25	48,15	0,09	0,62	0,29	24,14
3	-45	0	0,12	0,71	0,26	25,93	0,12	0,42	0,20	0,00
4	-30	0	0,09	0,46	0,17	0,00	0,08	0,30	0,07	0,00
5	-20	0	0,28	0,72	0,26	33,33	0,12	0,48	0,32	3,33
6	-12	-16	1,56	0,19	0,08	0,00	1,3	0,17	0,06	0,00
7	-12	16	0,06	0,30	0,08	0,00	0,06	0,26	0,09	0,00
8	-10	0	0,26	0,52	0,18	0,00	0,12	0,73	0,20	14,29
9	-6	-8	1,6	0,17	0,05	0,00	1,3	0,19	0,07	0,00
10	-6	8	0,08	0,30	0,10	0,00	0,07	0,27	0,12	0,00
11	-2	-20	2,8	0,12	0,07	0,00	2,4	0,09	0,05	0,00
12	0	-10	2,8	0,08	0,03	0,00	2,7	0,06	0,01	0,00
13	0	0	0,14	0,43	0,16	3,45	0,11	0,32	0,13	0,00

14	1	10	0,09	0,22	0,08	0,00	0,08	0,22	0,08	0,00
15	0	20	0,08	0,60	0,29	25,00	0,06	0,39	0,35	6,67
16	6	-8	1,05	0,61	0,19	3,85	0,93	0,41	0,14	0,00
17	6	8	0,07	0,24	0,10	0,00	0,06	0,21	0,06	0,00
18	10	0	0,11	0,56	0,19	0,00	0,1	0,44	0,19	0,00
19	12	-16	2,75	0,33	0,19	16,67	2,24	0,14	0,11	3,33
20	12	16	0,07	0,24	0,16	0,00	0,07	0,17	0,07	0,00
21	20	0	0,08	0,21	0,07	0,00	0,07	0,22	0,16	0,00
22	30	0	0,07	0,29	0,10	0,00	0,06	0,27	0,10	0,00
23	45	0	0,09	0,28	0,11	0,00	0,08	0,21	0,04	0,00
24	60	0	0,1	1,01	0,00	100.00	0,09	0,59	0,29	23,33
25	74	-2	0,1	1,01	0,00	100,00	0,08	0,96	0,12	76,92

Table 13. The target number and the corresponding horizontal and vertical eccentricities. The average luminance of the target's background (3°), the mean contrast threshold among the subjects and the standard deviation of the contrast thresholds, and the percentage of missed targets for both the original scene and the modified scene. 'High luminance' scene.

	high luminance		**Original scene**				**Modified scene**			
no	**h (deg)**	**v (deg)**	**L (cd/m2)**	**CT**	**σ**	**miss (%)**	**L (cd/m2)**	**CT**	**σ**	**miss (%)**
1	-75	0	0,22	0,99	0,06	91,7	0,18	0,93	0,15	66,67
2	-60	0	0,22	0,99	0,08	87,5	0,18	0,59	0,27	20,00
3	-45	0	0,27	0,77	0,28	46,2	0,24	0,54	0,21	6,67
4	-30	0	0,2	0,46	0,25	7,4	0,17	0,34	0,11	0,00
5	-20	0	0,66	0,72	0,27	33,3	0,26	0,49	0,21	3,33
6	-12	-16	3,83	0,22	0,13	0,0	3,34	0,18	0,08	0,00
7	-12	16	0,15	0,29	0,14	0,0	0,13	0,23	0,07	0,00
8	-10	0	0,61	0,68	0,22	13,3	0,26	0,67	0,23	3,33
9	-6	-8	4,24	0,20	0,15	0,0	3,2	0,17	0,05	0,00
10	-6	8	0,2	0,29	0,10	0,0	0,18	0,23	0,09	0,00
11	-2	-20	6,4	0,16	0,11	23,8	6,12	0,09	0,05	0,00
12	0	-10	7	0,07	0,03	0,0	6,32	0,07	0,02	0,00
13	0	0	0,39	0,32	0,09	0,0	0,26	0,32	0,19	0,00
14	1	10	0,21	0,31	0,15	0,0	0,19	0,22	0,08	0,00
15	0	20	0,17	0,54	0,29	24,1	0,14	0,31	0,12	0,00
16	6	-8	2,3	0,58	0,23	3,6	2,11	0,41	0,15	0,00
17	6	8	0,17	0,23	0,11	0,0	0,15	0,19	0,09	0,00
18	10	0	0,28	0,40	0,26	0,0	0,22	0,40	0,19	3,33
19	12	-16	5,75	0,27	0,13	42,9	5,36	0,16	0,09	0,00
20	12	16	0,16	0,23	0,18	0,0	0,15	0,17	0,07	0,00
21	20	0	0,21	0,21	0,07	0,0	0,19	0,17	0,05	0,00
22	30	0	0,16	0,25	0,10	0,0	0,14	0,24	0,09	0,00
23	45	0	0,2	0,27	0,20	3,6	0,18	0,24	0,11	0,00
24	60	0	0,23	1,00	0,03	96,2	0,19	0,69	0,29	33,33
25	74	-2	0,25	1,01	0,00	100,0	0,2	0,93	0,14	56,67

A definition for adaptation luminance is needed in order to implement the CIE 191:2010 system for mesopic photometry. The aim of this work was to analyse the adaptation luminance in street and road lighting environments. The focus was particularly on quantifying the increment or the decrement in the adaptation luminance, caused by luminance differences in the visual field. This was realised by examining the test subjects' contrast thresholds within visual fields, where the luminance distributions were non-uniform. Disability glare sources are the extreme instances of luminance non-uniformity. Their influence on the adaptation luminance was quantified by street environment luminance measurements and disability glare calculations.

Aalto-DD 172/2016

ISBN 978-952-60-6988-3 (printed)
ISBN 978-952-60-6987-6 (pdf)
ISSN-L 1799-4934
ISSN 1799-4934 (printed)
ISSN 1799-4942 (pdf)

Aalto University
School of Electrical Engineering
Department of Electrical Engineering and Automation
www.aalto.fi

BUSINESS + ECONOMY

ART + DESIGN + ARCHITECTURE

SCIENCE + TECHNOLOGY

CROSSOVER

DOCTORAL DISSERTATIONS